Nuclear Physics B345 (1990) 331–368
North-Holland

THE CONTRIBUTION OF THE GLUON–GLUON SUBPROCESS TO THE DRELL–YAN *K*-FACTOR

T. MATSUURA*

II. Institut für Theoretische Physik, Universität Hamburg, D-2000 Hamburg 50, FRG

R. HAMBERG and W.L. van NEERVEN**

Instituut-Lorentz, University of Leiden, P.O. Box 9506, 2300 RA Leiden, The Netherlands

Received 30 March 1990
(Revised 18 June 1990)

In this paper we present the calculation of the gluon–gluon contribution to the Drell–Yan *K*-factor. The size of the cross section for $g + g \to V + 'X'$ is compared with those coming from the three other subprocesses, i.e. $q + \bar{q} \to V + 'X'$, $q + g \to V + 'X'$ and $q + q \to V + 'X'$. Furthermore, the dependence of the *K*-factor on the factorization and renormalization scales is analyzed for the current and future colliders.

1. Introduction

During the last few years a great deal of progress has been made in calculating higher order corrections to inclusive and semi-inclusive processes in the framework of perturbative QCD [1]. At present it seems that most of the order α_s corrections to $n \to m$ parton reactions with $n + m \leqslant 4$ have been computed. An analysis of the existing calculations reveals that it will be very difficult to extend the radiative corrections beyond the first order in α_s. This in particular holds for semi-inclusive processes. This statement also applies to order α_s corrections to Born processes which involve more than four partons, like in multi-jet production.

However, in the case of inclusive processes the situation is a little better. An example is the quantity R defined in the reaction $e^+ + e^- \to X$, where X denotes any hadronic final state, which is now completely known up to order α_s^3 [2]. Another example is the order α_s^2 correction to the two-jet cross section of the same process [3]. Finally, we want to mention the *K*-factor in the Drell–Yan process for which a partial result exists at order α_s^2 [4].

* Supported by LAA, CERN, Geneva.
**Bitnet address: NEERVEN@HLERUL59

Higher order corrections are necessary for practical as well as theoretical reasons. The practical reason is that the statistics in the ongoing and future experiments will improve, so that higher order corrections will be measurable. This is expected, as the size of the various K- and R-factors can become rather large. Also it is interesting to see how the K-factors will behave at very large energies, which are characteristic of future accelerators like LHC and SSC. Here we expect that processes with gluons in the initial state will play a very important role. From the theoretical point of view higher order corrections are interesting because we can learn something about the behaviour of the perturbation series. In particular one wants to understand by which type of terms the series is dominated. An example is the soft gluon part of the K-factor, which can be traced back to reactions with one or more gluons in the final state. Furthermore, we expect that cross sections corrected to higher orders of α_s, are less sensitive to variations in the factorization and renormalization scales than the lowest order ones. In this paper we will study the effect of the order α_s^2 corrections to the Drell–Yan K-factor, corresponding to the total cross section for vector boson production.

The Drell–Yan process is given by the reaction

$$\begin{array}{l} H_1 + H_2 \to V + \text{hadronic states} \\ \qquad\qquad\quad \big\lfloor \to \ell_1 + \ell_2 \end{array} , \tag{1.1}$$

where V is a vector boson (W, Z or γ), which decays into a lepton pair (ℓ_1, ℓ_2). The four parton subprocesses contributing to the above are given by

$$q + \bar{q} \to V + \text{partons}, \tag{1.2}$$

$$q(\bar{q}) + g \to V + \text{partons}, \tag{1.3}$$

$$q(\bar{q}) + q(\bar{q}) \to V + \text{partons}, \tag{1.4}$$

$$g + g \to V + \text{partons}. \tag{1.5}$$

The quark–anti-quark subprocess is known in zeroth and first order in α_s [5–7], whereas a partial result exists in order α_s^2 [4]. The (anti)-quark–gluon subprocess shows up for the first time on the order α_s level. Its result can be found in refs. [5–7]. The lowest order cross section for the reactions (1.4) and (1.5) are already of order α_s^2. The result for the (anti)quark–(anti)quark subprocess is given in refs. [8, 9]. The gluon–gluon subprocess has not been calculated up to now. We will present the calculation of this process in sect. 2. In sect. 3 we study its contribution to the K-factor and compare it with the results for the other subprocesses. The dependence of the K-factor on the renormalization and factorization scales is also

studied. Furthermore, we make predictions for current and future accelerators. Details of the calculation and some useful formulae can be found in the appendices.

2. The gluon–gluon subprocess

The contribution of the gluon–gluon subprocess to the Drell–Yan cross section can be written as

$$\frac{\mathrm{d}\sigma^{gg}}{\mathrm{d}Q^2} = \tau\sigma_V \int_0^1 \mathrm{d}x \int_0^1 \mathrm{d}x_1 \int_0^1 \mathrm{d}x_2\, \delta(\tau - x x_1 x_2)\, g(x_1, M^2) g(x_2, M^2) \times C_V\, \Delta_{gg}(x, Q^2, M^2) \tag{2.1}$$

with

$$\tau = Q^2/S, \qquad C_\gamma = n_f \to \tfrac{4}{9}\,\mathrm{int}(n_f) + \tfrac{1}{9}\,\mathrm{int}\big(\tfrac{1}{2}(n_f+1)\big), \quad (2.2), (2.3)$$

$$C_Z = \Big(1 + \big[1 - \tfrac{8}{3}\sin^2\theta_W\big]^2\Big)\mathrm{int}\big(\tfrac{1}{2}n_f\big) + \Big(1 + \big[1 - \tfrac{4}{3}\sin^2\theta_W\big]^2\Big)\mathrm{int}\big(\tfrac{1}{2}(n_f+1)\big), \tag{2.4}$$

$$C_W = \mathrm{int}\big(\tfrac{1}{2}n_f\big). \tag{2.5}$$

In the above equations σ_V stands for the pointlike DY cross section. The kinematical variables Q^2 and S denote the di-lepton pair mass and the c.m. energy of the incoming hadrons, respectively. The gluon distribution function $g(x_i, M^2)$ depends on the mass factorization scale M. Furthermore, n_f is the number of flavours and θ_W the Weinberg angle. In this section we will discuss the calculation of the Drell–Yan correction term $\Delta_{gg}(x, Q^2)$.

In order α_s^2 the process under consideration is (see fig. 1)

$$g + g \to V + q + \bar{q}. \tag{2.6}$$

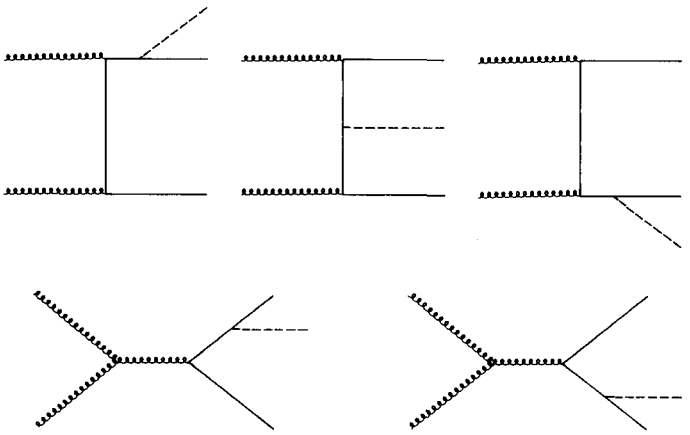

Fig. 1. The Feynman diagrams for the gluon–gluon subprocess.

The parton structure function $\hat{W}_{gg}$ of this process is given by

$$\hat{W}_{gg}(x, Q^2, \varepsilon) = A - C \int \mathrm{d}PS^{(3)} \sum M^{\mu} M_{\mu}^{\dagger}, \tag{2.7}$$

where

$$A = \frac{1}{4(N^2-1)^2}: \quad \text{averaging over gluon helicities and colours}, \tag{2.8}$$

$$C = \frac{-N}{2\pi(1+\frac{1}{2}\varepsilon)}: \quad \text{normalization factor}, \tag{2.9}$$

$$M^{\mu}: \quad \text{amplitude of the g–g process}. \tag{2.10}$$

The normalization factor C is due to the conventions introduced for the Born cross section. The summation in eq. (2.7) is over all the quantum numbers of M_{μ}. We use n-dimensional regularization to handle the collinear divergences ($\varepsilon = n - 4$). Notice that we have only averaged over the two physical helicity states of the gluon. Actually, using n-dimensional regularization one has to average over $(n-2)$ helicity states. This implies that eq. (2.8) and therefore also eqs. (2.12) and (2.13) have to be divided by a factor $(1+\frac{1}{2}\varepsilon)^2$ (two initial state gluons!). However, in the DIS scheme this is not necessary, because the mass factorization (see eq. (2.14)) involves products of parton structure functions which are obtained from subprocesses with one gluon in the initial state. Therefore, one has an overall factor $1/(1+\frac{1}{2}\varepsilon)^2$ in eq. (2.14), so that it does not matter whether the limit $\varepsilon \to 0$ is taken in this factor before or after mass factorization. Notice that in the literature [6, 7] one also has averaged over the two physical helicity states only. In the case of the $\overline{MS}$ mass factorization scheme, however, one has to include the factor $1/(1+\frac{1}{2}\varepsilon)^2$, since the helicity averaging factor does not appear in the splitting functions.

For the calculation it is convenient to divide the parton structure function $\hat{W}_{gg}$ into two colour parts

$$\hat{W}_{gg}(x, Q^2, \varepsilon) = \hat{W}_{gg}^{C_A}(x, Q^2, \varepsilon) + \hat{W}_{gg}^{C_F}(x, Q^2, \varepsilon), \tag{2.11}$$

where $\hat{W}_{gg}^{C_A}$ and $\hat{W}_{gg}^{C_F}$ correspond to the $C_A C_F$ and C_F^2 colour parts of the matrix element ($C_A = N$, $C_F = (N^2-1)/2N$, N = number of colours). After partial fractioning the phase space integration $\mathrm{d}PS^{(3)}$ has been performed in the c.m. frame of the incoming gluons. The calculational details can be found in appendix

A. We then find for the parton structure function $\hat{W}_{gg}(x, Q^2, \varepsilon)$

$$
\begin{aligned}
&\hat{W}_{gg}^{C_A}(x, Q^2, \varepsilon) \\
&\quad = \left(\frac{\alpha_s}{4\pi}\right)^2 \frac{N^2}{(N^2-1)} \left(\frac{Q^2}{4\pi\mu^2}\right)^{\varepsilon} \frac{\Gamma^2\left(1+\frac{1}{2}\varepsilon\right)}{\Gamma^2(1+\varepsilon)} x^{-\varepsilon}(1-x)^{2\varepsilon} \\
&\qquad \times \Big\{(1+x)^2\big[16 S_{1,2}(-x) + 24\,\mathrm{Li}_3(-x) + 16\zeta(3) - 24 \ln x\, \mathrm{Li}_2(-x) \\
&\qquad\qquad + 16 \ln(1+x)\mathrm{Li}_2(-x) + 8\ln(1+x)\zeta(2) - 12\ln^2 x \ln(1+x) \\
&\qquad\qquad + 8 \ln x \ln^2(1+x) + \tfrac{16}{3}\mathrm{Li}_2(-x) + \tfrac{8}{3}\zeta(2) + \tfrac{16}{3}\ln x \ln(1+x)\big] \\
&\qquad - 8(1-x)^2 S_{1,2}(1-x) + \left(\tfrac{50}{3}x^2 + \tfrac{4}{3}x - \tfrac{4}{3}\right)\ln^2 x \\
&\qquad - \left(50x^2 + \tfrac{76}{3}x + 4\right)\ln x + \tfrac{191}{3}x^2 - 48x - \tfrac{47}{3}\Big\}, \qquad (2.12)
\end{aligned}
$$

and

$$
\begin{aligned}
\hat{W}_{gg}^{C_F}(x, Q^2, \varepsilon) &= \left(\frac{\alpha_s}{4\pi}\right)^2 \left(\frac{Q^2}{4\pi\mu^2}\right)^{\varepsilon} \frac{\Gamma^2\left(1+\frac{1}{2}\varepsilon\right)}{\Gamma^2(1+\varepsilon)} x^{-\varepsilon}(1-x)^{2\varepsilon} \\
&\quad \times \Big\{ \frac{1}{\varepsilon^2}\big[-8(1+4x+4x^2)\ln x - 16(1+2x-3x^2)\big] \\
&\qquad + \frac{1}{\varepsilon}\big[-(1+4x+4x^2)\big(16\,\mathrm{Li}_2(1-x) + 4\ln^2 x\big) \\
&\qquad\quad - (20+32x)\ln x - 86x^2 + 88x - 2\big] \\
&\qquad - 8(11x^2+14x+2) S_{1,2}(1-x) - 16(1+x)^2 S_{1,2}(-x) \\
&\qquad + 32(4x^2+4x+1)\mathrm{Li}_3(1-x) + 8(x^2-2x-1)\mathrm{Li}_3(-x) \\
&\qquad + 4(2x^2-2x-1)\zeta(3) - 20(4x^2+4x+1)\ln x\, \mathrm{Li}_2(1-x) \\
&\qquad + 8(x^2+4x+2)\ln x\, \mathrm{Li}_2(-x) + 4(10x^2+10x+3)\ln x \zeta(2) \\
&\qquad - 16(1+x)^2 \ln(1+x)\mathrm{Li}_2(-x) - 8(1+x)^2 \ln(1+x)\zeta(2) \\
&\qquad - \tfrac{8}{3}(3x^2+3x+1)\ln^3 x + 12(1+x)^2 \ln^2 x \ln(1+x) \\
&\qquad - 8(1+x)^2 \ln x \ln^2(1+x) + 8(3x^2-10x-6)\mathrm{Li}_2(1-x) \\
&\qquad + 8(1+x)\mathrm{Li}_2(-x) + 4(-12x^2+9x+5)\zeta(2) \\
&\qquad - (12x^2+22x+15)\ln^2 x + 8(1+x)\ln x \ln(1+x) \\
&\qquad + (38x^2+4x-15)\ln x + \tfrac{267}{2}x^2 - 128x - \tfrac{11}{2}\Big\}, \qquad (2.13)
\end{aligned}
$$

where μ^2 is an artefact of the n-dimensional regularization, which can be traced back to the dimensionality of the coupling constant. Notice that $\hat{W}_{gg}^{C_A}$ is free of mass singularities; only the C_F^2 part of $\hat{W}_{gg}$ contains collinear divergences. To handle these divergences we perform mass factorization in the DIS scheme. In this scheme the contribution of the gluon–gluon subprocess to the Drell–Yan correction term is given by

$$\Delta_{gg}(x,Q^2) = \hat{W}_{gg}(x,Q^2,\varepsilon) + \tfrac{1}{2}\big(\hat{\mathscr{F}}_2^{(1),g} \otimes \hat{\mathscr{F}}_2^{(1),g}\big)(x,Q^2,\varepsilon) - 2\big(\hat{\mathscr{F}}_2^{(1),g} \otimes \hat{W}_{qg}^{(1)}\big)(x,Q^2,\varepsilon), \tag{2.14}$$

where $\hat{\mathscr{F}}_2^{(1),g}$ and $\hat{W}_{qg}^{(1)}$ are the parton structure functions belonging to the deep inelastic scattering process $V + g \to q + \bar{q}$ and the Drell–Yan process $q + g \to V + q$, respectively [6, 7]. Furthermore, the symbol $\otimes$ denotes the convolution, i.e.

$$(f \otimes g)(x) = \int_0^1 dy \int_0^1 dz\, \delta(x - yz) f(y) g(z). \tag{2.15}$$

Dividing the Drell–Yan correction Δ_{gg} also into two colour parts, we have

$$\Delta_{gg}(x,Q^2) = \Delta_{gg}^{C_A}(x,Q^2) + \Delta_{gg}^{C_F}(x,Q^2) \tag{2.16}$$

with (see eq. (2.12))

$$\Delta_{gg}^{C_A}(x,Q^2) = \hat{W}_{gg}^{C_A}(x,Q^2,\varepsilon = 0) \tag{2.17}$$

and

$$\begin{aligned}
\Delta_{gg}^{C_F}(x,Q^2) = \left(\frac{\alpha_s}{4\pi}\right)^2 \Big\{ & -4(10x^2+16x+1)S_{1,2}(1-x) - 16(1+x)^2 S_{1,2}(-x) \\
& + 4(4x^2+4x+1)\mathrm{Li}_3(1-x) + 8(x^2-2x-1)\mathrm{Li}_3(-x) \\
& + 4(2x^2-2x-1)\zeta(3) - 6(4x^2+4x+1)\ln x\, \mathrm{Li}_2(1-x) \\
& + 8(x^2+4x+2)\ln x\, \mathrm{Li}_2(-x) - 4(4x^2+4x+1)\ln(1-x)\, \mathrm{Li}_2(1-x) \\
& - 16(1+x)^2 \ln(1+x)\mathrm{Li}_2(-x) - 8(1+x)^2 \ln(1+x)\zeta(2) \\
& - \left(4x^2+4x+\tfrac{5}{3}\right)\ln^3 x + 12(1+x)^2 \ln^2 x \ln(1+x) \\
& - 2(4x^2+4x+1)\ln x \ln^2(1-x) - 8(1+x)^2 \ln x \ln^2(1+x) \\
& + (16x^2+16x+6)\ln x \zeta(2) - (6x^2+10x+7)\ln^2 x \\
& - 6(8x^2+8x+1)\ln x \ln(1-x) + 8(1+x)\ln x \ln(1+x) \\
& + 4(3x^2-2x-1)\ln^2(1-x) - (12x^2+72x+18)\mathrm{Li}_2(1-x) \\
& + 8(1+x)\mathrm{Li}_2(-x) + (-12x^2+12x+8)\zeta(2) - (26x^2+96x+24)\ln x \\
& + (51x^2-36x-15)\ln(1-x) + \tfrac{83}{2}x^2 - 5x - \tfrac{73}{2}\Big\}.
\end{aligned} \tag{2.18}$$

3. The results

First we will introduce some notations which will be helpful for the discussion of our results. Generalizing eq. (2.1) the colour-averaged cross section of the process in eq. (1.1) is given by

$$\mathrm{d}\sigma/\mathrm{d}Q^2 = \tau\sigma_{\mathrm{V}}(Q^2, M_{\mathrm{V}}^2)W_{\mathrm{V}}(\tau, Q^2), \tag{3.1}$$

where, according to the DY mechanism, the hadronic structure function $W_{\mathrm{V}}(\tau, Q^2)$ can be written as

$$W_{\mathrm{V}}(\tau, Q^2) = \sum_{i,j} \int_0^1 \mathrm{d}x \int_0^1 \mathrm{d}x_1 \int_0^1 \mathrm{d}x_2\, \delta(\tau - xx_1x_2)\mathrm{PD}_{\mathrm{V}}^{ij}(x_1, x_2, M^2)$$

$$\times \Delta_{ij}(x, Q^2, M^2). \tag{3.2}$$

The function $\mathrm{PD}_{\mathrm{V}}^{ij}(x_1, x_2, M^2)$ is the usual combination of parton distribution functions, which depends on the mass factorization scale M^2. The indices i and j refer to the type of the incoming partons. Moreover, it contains all the information on the coupling of the quarks to the vector bosons, such as the quark charges, the Weinberg angle θ_{W} and the Cabibbo angle θ_{C} (the other angles and phases of the CKM matrix are neglected). The total cross section σ for W/Z-production is obtained by integrating eq. (3.1) over Q^2 using the narrow width approximation. Therefore, the relevant mass scale will be $Q^2 = M_{\mathrm{V}}^2$ (M_{V} is the mass of the vector boson).

Notice that the parton distribution functions do not only depend on the mass factorization scale M, but also on the renormalization scale R. This is because the calculation of the anomalous dimension involves the operator renormalization (= mass factorization) as well as the coupling constant renormalization. However, in the existing parametrizations of the parton distribution functions the two scales M and R are put equal. Also the DY correction term $\Delta_{ij}(x, Q^2, M^2)$ (Wilson coefficient) depends on these two scales. This can be seen by expanding the DY correction term in a power series in the running coupling constant $\alpha_{\mathrm{s}}(R^2)$

$$\Delta_{ij}(x, Q^2, M^2) = \sum_{n=0}^{\infty} \alpha_s^n(R^2)\Delta_{ij}^{(n)}(x, Q^2, M^2, R^2). \tag{3.3}$$

If $\alpha_{\mathrm{s}}(R^2)$ is expanded in a power series in $\alpha_{\mathrm{s}}(M^2)$ the explicit R^2-dependence in eq. (3.3) drops out.

The parton distribution functions as well as the DY correction term are scheme dependent. In our calculations the mass factorization has been performed in the DIS scheme, whereas the renormalized coupling constant is determined in the $\overline{MS}$ scheme. Therefore, one has to choose an appropriate parametrization for the

distribution functions in the DIS scheme. We will use the DFLM (set-4) parametrization [10] for our main computations. However, in order to check its reliability at high energy colliders, like the LHC and SSC, we also have done some of our numerical calculations with the leading log parametrizations DO1 [11] and EHLQ [12]. For the running coupling constant we take the two-loop corrected one defined in the $\overline{MS}$ scheme [13].

In the presentation of our tables and figures we have used all expressions for the various DY correction terms Δ_{ij}, which are known up to now, including the one calculated in sect. 2. Starting with the reaction in eq. (1.2), $\Delta_{q\bar{q}}$ receives contributions from the processes

$$\Delta^{(0)}_{q\bar{q}}: \quad q + \bar{q} \to V \tag{3.4a}$$

$$\Delta^{(1)}_{q\bar{q}}: \quad q + \bar{q} \to V + g, \tag{3.4b}$$

$$\Delta^{(2)}_{q\bar{q}}: \quad \begin{cases} q + \bar{q} \to V + g + g \\ q + \bar{q} \to V + q + \bar{q} \end{cases}, \tag{3.4c}$$

$$\Delta^{(2)}_{q\bar{q},S}: \quad q + \bar{q} \to V + q + \bar{q}. \tag{3.4d}$$

We have divided the contribution of the subprocess $q + \bar{q} \to V + q + \bar{q}$ into two parts. The first one ($\Delta^{(2)}_{q\bar{q}}$) shows up in both the singlet and the non-singlet contribution to the DY correction term. The second part ($\Delta^{(2)}_{q\bar{q},S}$) appears in the singlet contribution only. The above reactions also include the virtual corrections to the processes in eqs. (3.4a) and (3.4b). The correction terms can be found in the literature [4–7], except for the hard gluon contribution to (3.4c) and a part of process (3.4d), which have not been calculated yet. The known part of $\Delta_{q\bar{q},S}$ is equal to Δ_{qq} (see below) without the identical quark contribution.

Following the notation of ref. [14] we can split $\Delta^{(i)}_{q\bar{q}}$ into a "soft + virtual" (S + V) and a hard (H) gluon part. The structure of the (S + V) part is given by

$$\begin{aligned} &\Delta^{(S+V)}_{q\bar{q}}(x, Q^2, M^2, R^2) \\ &\quad = \delta(1-x) + \sum_{n=1}^{\infty} \left(\frac{\alpha_s(R^2)}{4\pi} \right)^n \\ &\qquad \times \left[\sum_{i=0}^{2n-1} a_{ni}(Q^2, M^2, R^2) \mathscr{D}_i(x) + b_n(Q^2, M^2, R^2) \delta(1-x) \right]. \end{aligned} \tag{3.5}$$

The coefficients a_{ni} and b_n can be found in refs. [4] and appendix C. The hard gluon part $\Delta^{H}_{q\bar{q}}$ does not contain distributions of the types shown in eq. (3.5). Its expression for the second process in eq. (3.4c) can be found in ref. [15].

The DY correction term for reaction (1.3) is only known in lowest order [5–7]. It will be denoted by

$$\Delta_{qg}^{(1)}: \quad q(\bar{q}) + g \to V + q(\bar{q})\,. \tag{3.6}$$

In sect. 2 we have calculated the correction term due to the gluon–gluon fusion process

$$\Delta_{gg}^{(2)}: \quad g + g \to V + q + \bar{q}\,. \tag{3.7}$$

Finally, the correction term for the subprocess

$$\Delta_{qq}^{(2)}: \quad q(\bar{q}) + q(\bar{q}) \to V + q(\bar{q}) + q(\bar{q}) \tag{3.8}$$

can be found for identical as well as non-identical quarks in refs. [8, 9] (see also appendix B). Besides the general structure of the (S + V) part of $\Delta_{q\bar{q}}$, we found that the functions $\Delta_{q\bar{q},S}^{(2)}$, $\Delta_{gg}^{(2)}$ and $\Delta_{qq}^{(2)}$ vanish in the limit $x \to 1$. This feature explains why the contributions of the processes (3.4d), (3.7) and (3.8) are very small at the current and future accelerators, as we will see below. Notice that this property is scheme independent since any finite mass factorization involves only convolutions of regular functions which vanish in the limit $x \to 1$. Contrary to the corrections terms mentioned above, $\Delta_{q\bar{q}}^{H}$ and Δ_{qg} do not vanish for $x = 1$, so that their contributions become appreciable in particular at very high ($\sqrt{S} \geqslant 16$ TeV) energies.

We will now present the Drell–Yan cross section and its K-factor for both pp and p$\bar{\text{p}}$-colliders. The input parameters are $M_Z = 91$ GeV, $M_W = 80$ GeV, $\sin^2\theta_W = 0.227$ and $\sin^2\theta_C = 0.05$. The number of light flavours, n_f, is taken to be equal to five. The QCD scale parameter Λ, which appears in both the running coupling constant and the parton distribution functions is chosen to be 0.2 GeV. Unless stated differently all the results are produced using the DFLM (set-4) parametrization [10]. Furthermore, we take $M = R = M_V$ (M_V is the vector boson mass). The stability of the cross sections under changes of the mass factorization and renormalization scales will be presented at the end of this section. All the numerical results in this paper are produced by our FORTRAN program ZWPROD, which can be obtained on request.

Starting with the Z-production at p$\bar{\text{p}}$-colliders we show in fig. 2 the zeroth order (σ_0), the $O(\alpha_s)$ corrected (σ_1) and the $O(\alpha_s^2)$ corrected (σ_2) DY cross section for $0.5\ \text{TeV} \leqslant \sqrt{S} \leqslant 50$ TeV. From this figure we infer that σ_i increases logarithmically as a function of $\sqrt{S}$. This is not surprising since at large S (small τ) the sea quarks dominate the process and their distribution functions behave like $\sim 1/x$ for $x \to 0$. For the discussion of the various contributions to the Drell–Yan correction term it

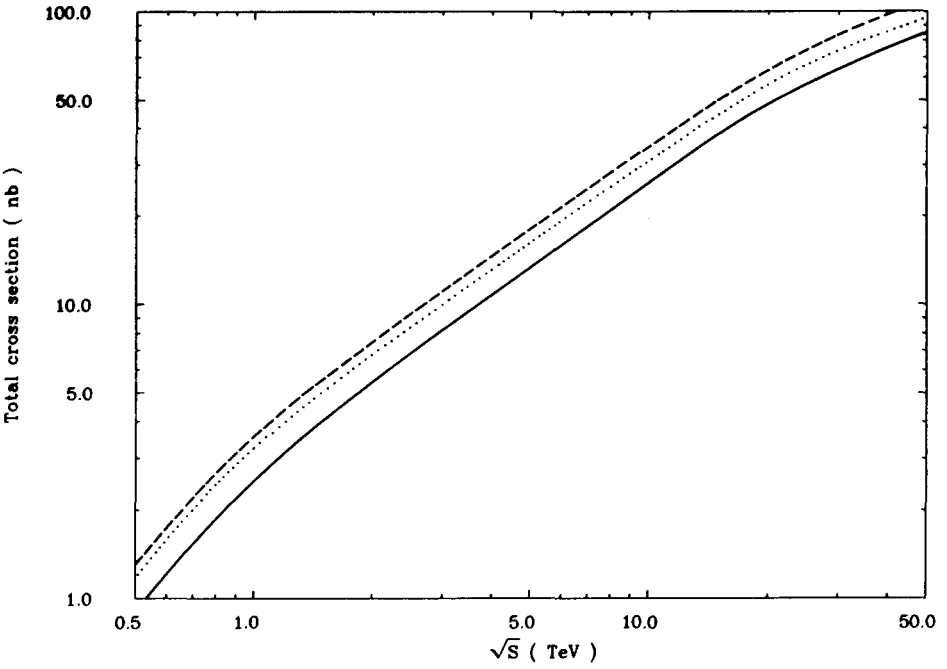

Fig. 2. The total cross section for the Z-production at a $p\bar{p}$-collider in three approximations. Solid line: Born; dotted line: $O(\alpha_s)$ corrected; dashed line: $O(\alpha_s^2)$ corrected.

is convenient to introduce the K-factor. It is defined by

$$K_{\text{th}} = \sum_{n=0}^{\infty} K^{(n)}, \tag{3.9}$$

where $K^{(n)}$ is the $O(\alpha_s^n)$-contribution to the theoretical K-factor, which is given by

$$K^{(n)} = \frac{W^{(n)}(\tau, Q^2)}{W^{(0)}(\tau, Q^2)}. \tag{3.10}$$

The function $W^{(n)}(\tau, Q^2)$ is the order α_s^n term of the hadronic structure function $W_V(\tau, Q^2)$ in eq. (3.2). The order α_s^i corrected K-factor follows from eqs. (3.9) and (3.10) and it equals

$$K_i = \sum_{n=0}^{i} K^{(n)}. \tag{3.11}$$

In fig. 3 one observes a slow decrease of K_1 and K_2. In K_2 the decrease due to $K^{(1)}$ is somewhat compensated by an increase of $K^{(2)}$. The latter becomes even

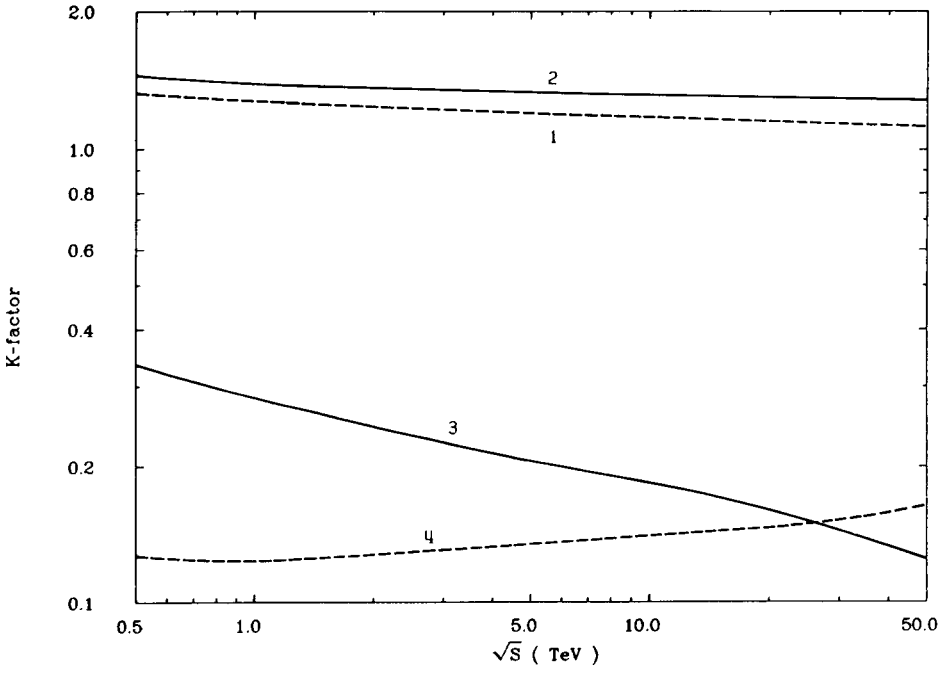

Fig. 3. The K-factor for the Z-production at a $p\bar{p}$-collider (see eqs. (3.10) and (3.11)). (1): K_1, (2): K_2, (3): $K^{(1)}$, (4): $K^{(2)}$.

larger than $K^{(1)}$ for $\sqrt{S} \geqslant 25$ TeV. In particular this implies that at SSC energies the $O(\alpha_s^2)$-corrections are larger than the $O(\alpha_s)$ ones*. The reason for this effect can be seen in fig. 4. Here we have split $K^{(n)}$ into the various contributions coming from the different production mechanisms in eqs. (3.4a)–(3.8). We observe that the $q\bar{q}$-process (i.e. $K^{(1)}_{q\bar{q}}$ and $K^{(2)}_{q\bar{q}}$) dominates the theoretical K-factor. However, at very large energies we see a steep rise of $K^{(1)}_{qg}$ (quark–gluon subprocess) becoming larger than $K^{(2)}_{q\bar{q}}$. Notice that the contribution of the quark–gluon process is negative, therefore it is responsible for the decrease of $K^{(1)}$, observed in fig. 3. At first sight the rapid growth of the qg-contribution is not surprising since the vector boson production at very large energies implies very small $\tau = x_1 x_2 = M_V^2/S$. Near $x_i = 0$ the gluon distribution function rises very steeply, so we expect that the gluons will give a very important contribution to the DY cross section. However, the large size of $K^{(1)}_{qg}$ is not only due to the gluon distribution function. If that would be the case, we would also have a sizeable contribution from the gluon–gluon subprocess (eq. (3.7)) calculated in this paper. A quick glance at fig. 4 shows that

* This we find in the approximation used here. The complete $K^{(2)}$ might behave differently. See the discussion of $K^{(2)}_{qg}$ below.

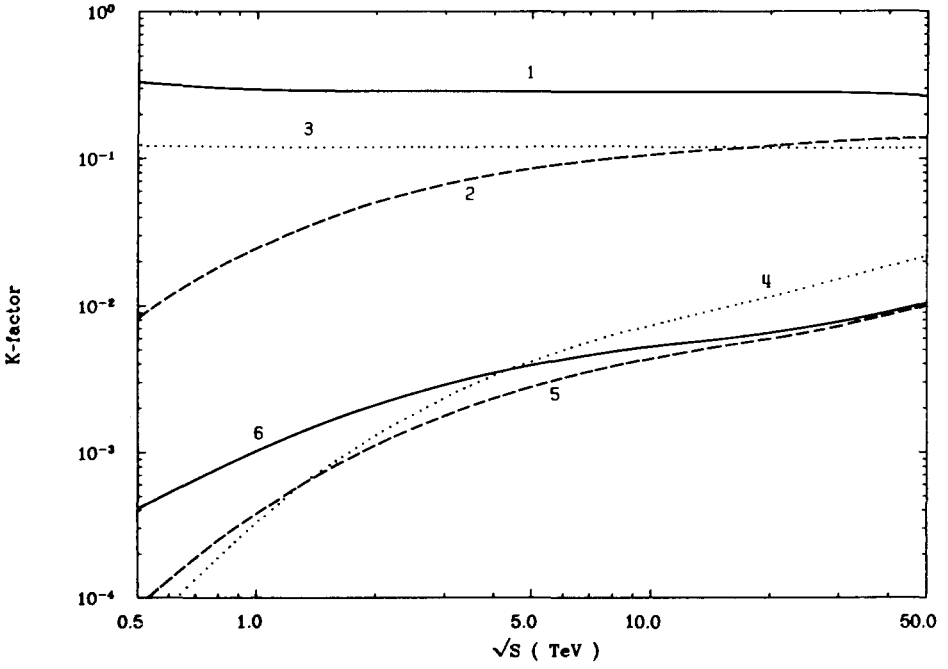

Fig. 4. The various contributions to the K-factor for the Z-production at a $p\bar{p}$-collider (see eq. (3.10). (1): $K^{(1)}_{q\bar{q}}$, (2): $-K^{(1)}_{qg}$, (3): $K^{(2)}_{q\bar{q}}$, (4): $K^{(2)}_{gg}$, (5): $K^{(2)}_{qq}$, (6): $K^{(2)}_{q\bar{q},S}$.

this is not the case. To understand this we rewrite eq. (3.2) as follows

$$W_V(\tau, Q^2) = \sum_{i,j} \int_\tau^1 \frac{dx}{x} \Phi_{ij}(x, M^2) \Delta_{ij}\left(\frac{\tau}{x}, Q^2, M^2\right), \tag{3.12}$$

where Φ_{ij} denotes the parton flux

$$\Phi_{ij}(x, M^2) = \int_x^1 \frac{dy}{y} \mathrm{PD}_{ij}\left(y, \frac{x}{y}, M^2\right). \tag{3.13}$$

It appears that for all subprocesses the flux $\Phi_{ij}(x, M^2)$ gets very large for $x \to 0$, whereas it goes rapidly to zero when $x \to 1$. Hence the behaviour of $\Delta_{ij}(x)$ in the limit $x \to 1$ is very important. As mentioned below eq. (3.8), it turns out that the DY correction terms $\Delta^{(2)}_{qq,S}$, $\Delta^{(2)}_{gg}$ and $\Delta^{(2)}_{qq}$ vanish in this limit, which explains their rather small contribution (less than 1%) to the total Drell–Yan K-factor. This is clearly shown in fig. 4. However, $\Delta^{(1)}_{qg}$ does not go to zero for $x \to 1$. It even diverges logarithmically. The same holds for $\Delta^{(1),H}_{q\bar{q}}$ and the known part of $\Delta^{(2),H}_{q\bar{q}}$. For this reason we show in fig. 5 the contributions from the "soft + virtual" and

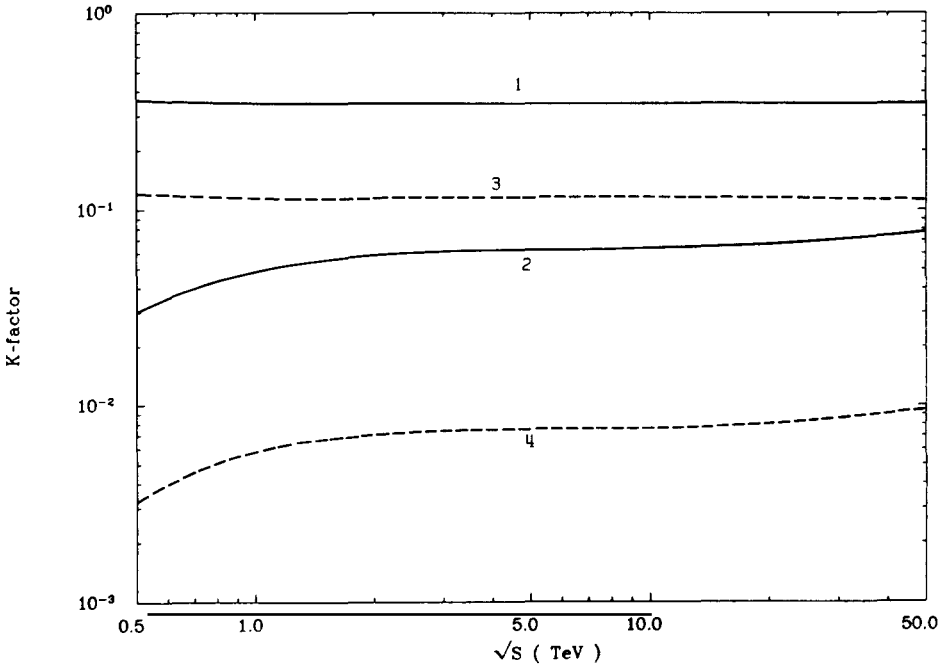

Fig. 5. The "soft + virtual" and hard gluon parts of $K_{q\bar{q}}^{(i)}$ for the Z-production at a $p\bar{p}$-collider (see eq. (3.6)). (1): $K_{q\bar{q}}^{(1),(S+V)}$, (2): $-K_{qq}^{(1),H}$, (3): $K_{q\bar{q}}^{(2),(S+V)}$, (4): $K_{q\bar{q}}^{(2),H}$.

hard gluon parts of $\Delta_{q\bar{q}}$ separately. We observe that although the (S + V) part dominates the hard gluon contribution over the whole energy range, the hard (H) gluon piece is not completely negligible. This holds for both $K_{q\bar{q}}^{(1)}$ and $K_{q\bar{q}}^{(2)}$. One also has to bear in mind that the complete hard gluon contribution to $K_{q\bar{q}}^{(2)}$ is not known yet. The same applies to $K_{qg}^{(2)}$. In the light of the discussion above it is not improbable that for high energy colliders the missing parts will give appreciable contributions to the DY K-factor, for they will have the same behaviour near $x = 1$ as the lower order DY correction terms $\Delta_{q\bar{q}}^{(1),H}$ and $\Delta_{qg}^{(1)}$.

The above discussion also holds for Z-production at pp-colliders, as can be seen in figs. 6–9. Because the same applies to W-production at proton–(anti)proton colliders, in these cases we only give the figures for the total cross section (see figs. 10 and 11).

Notice that there is a difference between W^+ and W^- production for pp-collisions. At low energies the valence quarks dominate the $q\bar{q}$ cross section, where W^+ and W^- are produced via u_V-sea and d_V-sea annihilation, respectively. The dominance of the valence quarks also explains the difference in vector boson production at pp- and $p\bar{p}$-colliders. However, at very large energies the sea quarks determine the cross section, so that the above-mentioned differences disappear.

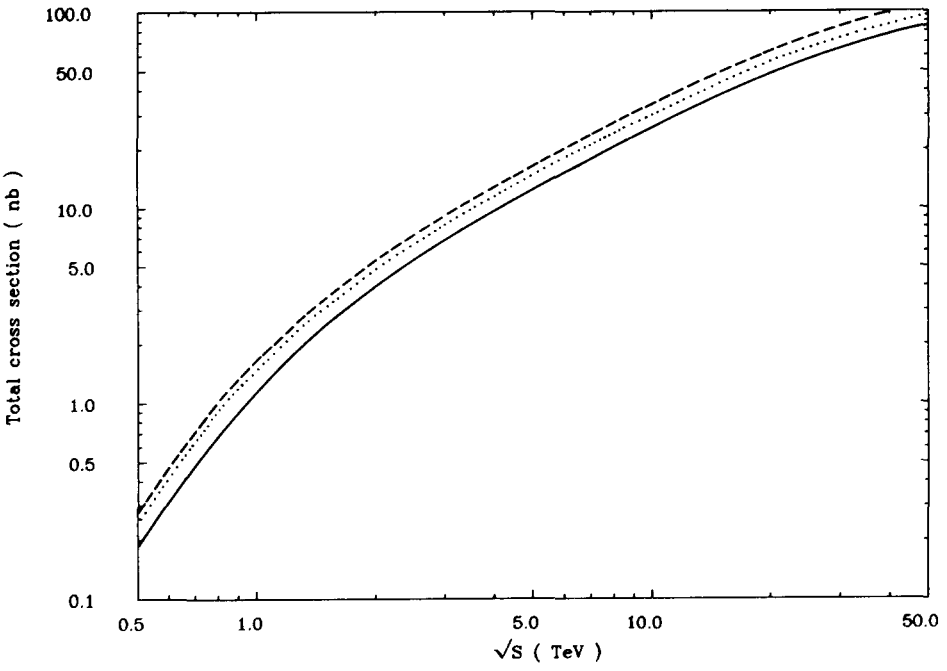

Fig. 6. The total cross section for the Z-production at a pp-collider in three approximations. Solid line: Born; dotted line: $O(\alpha_s)$ corrected; dashed line: $O(\alpha_s^2)$ corrected.

The size of the various contributions to the DY cross section depends very heavily on the specific set of parton distribution functions. These functions are extracted from the deep inelastic lepton–hadron scattering data, which are taken at $x \geqslant 0.01$. However, vector boson production at future, high energy colliders requires the knowledge of these distributions at $x \sim M_V/\sqrt{S}$. For LHC and SSC this implies $x \sim 6 \times 10^{-3}$ and $x \sim 3 \times 10^{-3}$, respectively. Therefore, we have to extrapolate the parton distribution functions to x-regions, which were not accessible to the deep inelastic experiments carried out up to now. In the future this situation will improve, when the HERA machine is put into operation. At this moment the only way to estimate the accuracy of our predictions is to compare the results obtained for different sets of distribution functions available in the literature. Here we have chosen the sets DO1 [11] and EHLQ [12], which will be compared with DFLM4 [10] used above.

The results for Z-production are displayed in table 1 for $\sqrt{S} = 0.63$ TeV ($p\bar{p}$, $Sp\bar{p}S$), 1.8 TeV ($p\bar{p}$, Tevatron), 16 TeV (pp, LHC) and 40 TeV (pp, SSC). The agreement between the three sets is excellent at $\sqrt{S} = 0.63$ TeV. They start to deviate from each other at $\sqrt{S} = 1.8$ TeV. However, the differences are still smaller than the $O(\alpha_s^2)$ correction. This situation changes, if we go to LHC and SSC

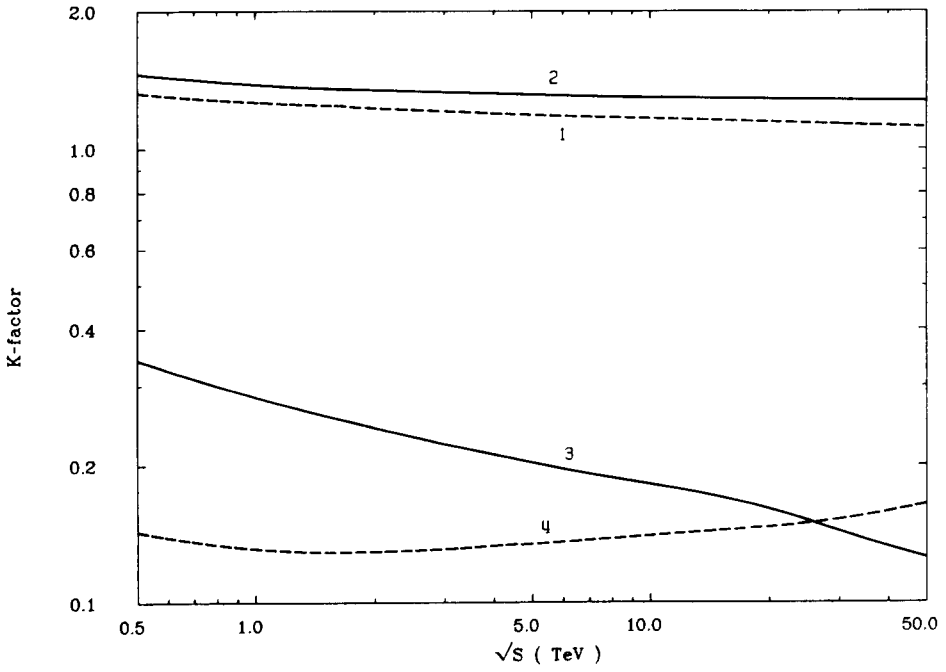

Fig. 7. The K-factor for the Z-production at a pp-collider (see eqs. (3.10) and (3.11)). (1): K_1, (2): K_2, (3): $K^{(1)}$, (4): $K^{(2)}$.

energies, where the differences between the three sets are of the same order or even larger than the $O(\alpha_s)$ corrections. Notice that the results for the three sets start to diverge already at the Born level and that adding higher order correction does not change the situation appreciably.

In table 2 we present the $O(\alpha_s)$ and $O(\alpha_s^2)$ radiatively corrected cross sections for $W^{\pm}$ production at the same energies as mentioned above. Here the deviation between the three parametrizations starts already at $\sqrt{S} = 0.63$ TeV. This is mainly due to the valence part of the d-quark distribution, which is more important for W than for Z-production.

From the two tables we infer that the EHLQ set leads to a considerably smaller cross section than those obtained from the other two sets. At the SSC energy the DO1 set gives a result, which is larger by more than 25% than found for the two other ones. Summarizing the above we can state that the uncertainty in the cross sections can be estimated to be up to 20% for LHC and 30% for SSC energies. It is for this reason that in studying radiative corrections it is better to look at the K-factor than at the cross section, since the uncertainty in the latter will drop out in the ratio of eq. (3.10).

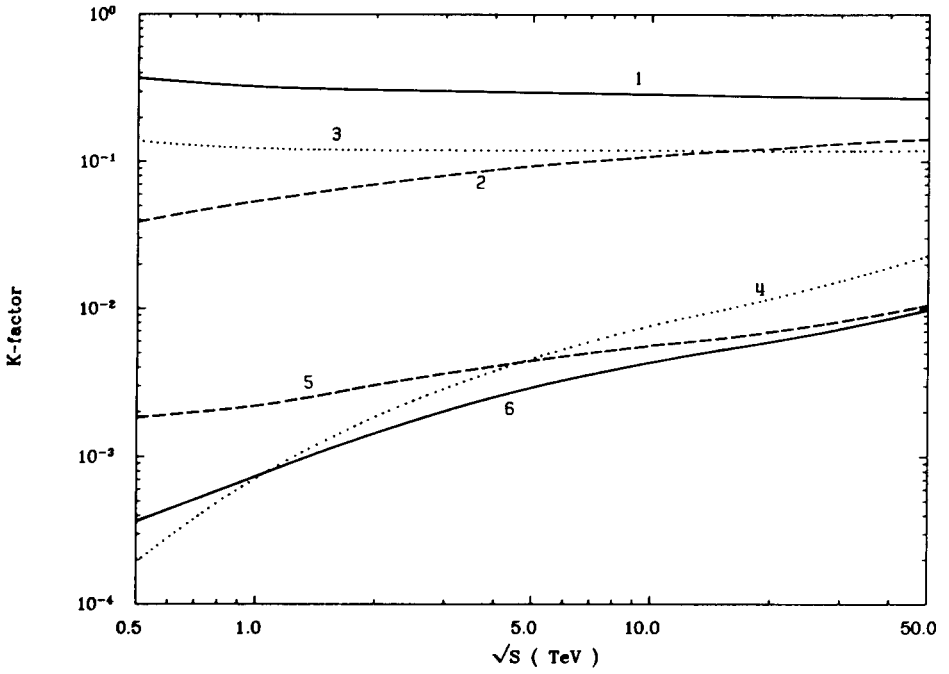

Fig. 8. The various contributions to the K-factor for the Z-production at a pp-collider (see eq. (3.10)). (1): $K^{(1)}_{q\bar{q}}$, (2): $-K^{(1)}_{qg}$, (3): $K^{(2)}_{q\bar{q}}$, (4): $K^{(2)}_{gg}$, (5): $K^{(2)}_{qq}$, (6): $K^{(2)}_{q\bar{q},S}$.

In tables 1 and 2 we also give the sum of the contributions from the hard gluon part of the first order $q\bar{q}$ ($\Delta^{(1),H}_{q\bar{q}}$) and the qg subprocess ($\Delta^{(1)}_{qg}$) separately. The results are put between brackets behind the $O(\alpha_s)$-corrected cross section. From these tables it is clear that the contribution from this sum increases rapidly with the c.m. energy of the collider, viz. from -6% of the Born cross section at $\sqrt{S} = 0.63$ TeV to around -25% at $\sqrt{S} = 40$ TeV. Moreover, from figs. 4, 5, 8 and 9 one can infer that this growth is mainly due to the qg-subprocess. Therefore we expect that $\Delta^{(2)}_{qg}$, which has not been calculated yet, will give a non-negligible contribution to the cross section at large energies. The same holds to a lesser extent for the hard part of $\Delta^{(2)}_{q\bar{q}}$.

For $\sqrt{S} = 0.63$ and 1.8 TeV (CERN and FNAL) we compare our predictions with the measurements by the UA2 [16] and CDF [17] collaborations (see tables 3 and 4). For this purpose one has to multiply the results obtained in tables 1 and 2 by the branching ratios BR($Z \to e^+e^-$)* and BR($W \to e\nu$) [19], respectively. We find that for the Z-production at CERN one needs the second order contributions to get an agreement between theory and experiment. For the other cases this

* This branching ratio is calculated using the program ZSHAPE [18].

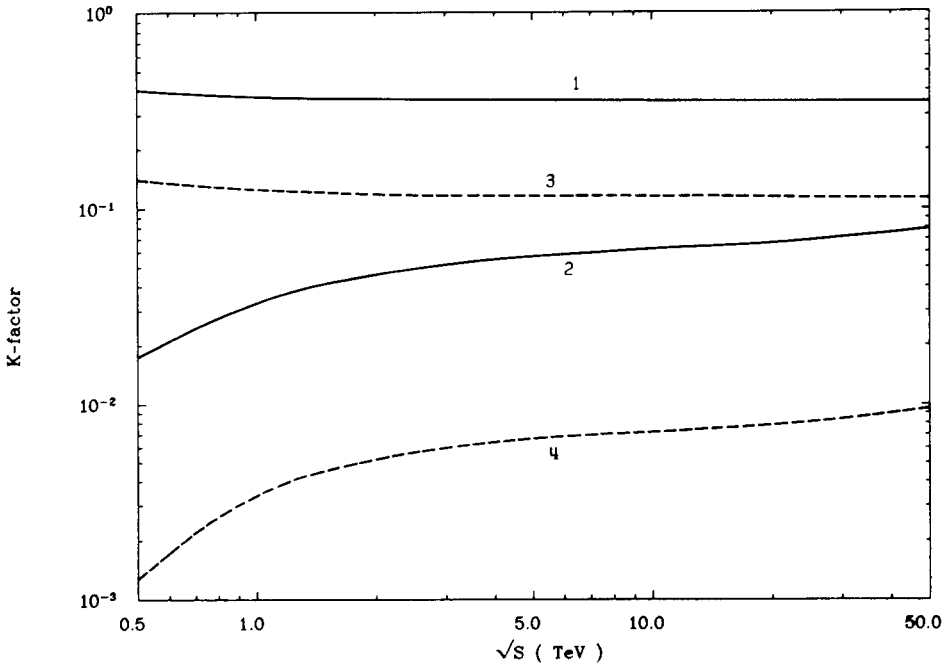

Fig. 9. The "soft + virtual" and hard gluon parts of $K_{q\bar{q}}^{(i)}$ for the Z-production at a pp-collider (see eq. (3.6)). (1): $K_{q\bar{q}}^{(1),(S+V)}$, (2): $-K_{q\bar{q}}^{(1),H}$, (3): $K_{q\bar{q}}^{(2),(S+V)}$, (4): $K_{q\bar{q}}^{(2),H}$.

statement is no longer true. At Tevatron even the Born approximation agrees with the measurements.

Finally, we are interested in the stability of our results if the mass factorization scale M and the renormalization scale R deviate from the "natural" ones, i.e. if one no longer has $M = R = M_V$. For this purpose we study the quantity

$$S_n(M_V^2, M^2, R^2) = \frac{\sigma_n(Q^2 = M_V^2, M^2, R^2)}{\sigma_n(Q^2 = M_V^2, M_V^2, M_V^2)}, \tag{3.14}$$

where σ_n denotes the $O(\alpha_s^n)$-corrected cross section. In tables 5–8 we present the values for S_n at $\sqrt{S} = 0.63$, 1.8, 16 and 40 TeV in the case of Z-production. Since the functions S_n for $W^{\pm}$-production exhibit the same behaviour, we do not show them separately. Notice that the results have been obtained for the DFLM set only. In this set the scale dependence of the parton distribution functions is determined by the next to leading order anomalous dimension. The second order anomalous dimension also shows up in the $O(\alpha_s^2)$ corrected DY Wilson coefficient $\Delta(x, Q^2, M^2)$. Therefore we expect that the $O(\alpha_s^2)$-corrected cross section becomes less dependent on the parameters M and R than the $O(\alpha_s)$ one. Notice that the DY cross section is less sensitive to scale variations than reactions like direct photon production [20] or heavy flavour production [21]. In lowest order the DY

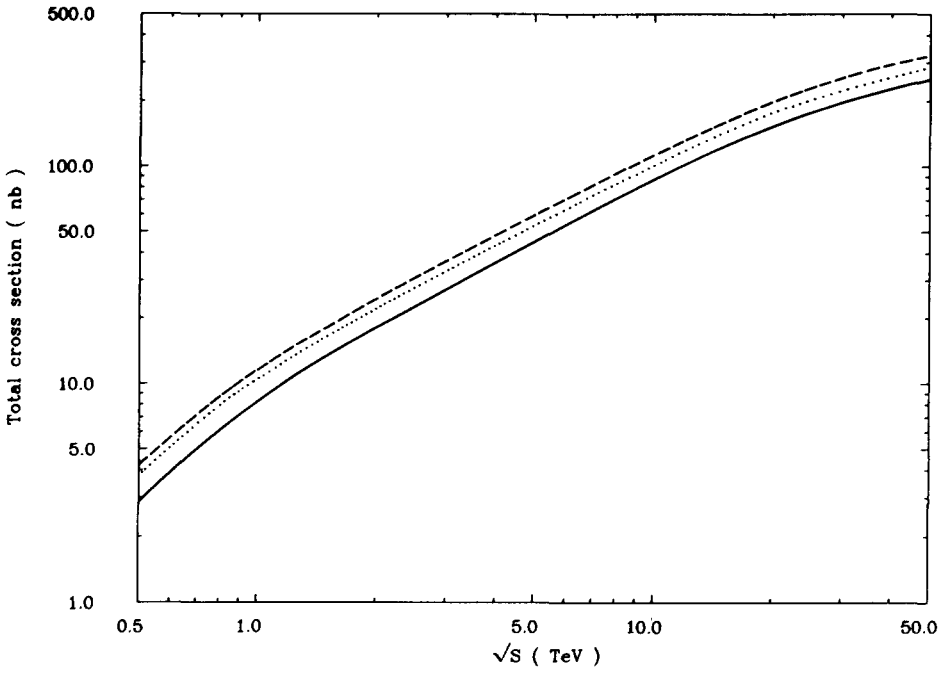

Fig. 10. The total cross section for the $W^+ + W^-$ production at a $p\bar{p}$-collider in three approximations. Solid line: Born; dotted line: $O(\alpha_s)$ corrected; dashed line: $O(\alpha_s^2)$ corrected.

cross section is independent of α_s, whereas the other two start at α_s and α_s^2, respectively. If a cross section at lowest order is proportional to α_s or α_s^2, it is very sensitive to variations in the renormalization scale, which will only be partially compensated by higher order corrections.

Our results have to be interpreted with some care and that for the following reasons. Firstly, we only take into account a part of the $O(\alpha_s^2)$-corrections and neglect the contributions $\Delta_{qg}^{(2)}$ and $\Delta_{q\bar{q}}^{(2),H}$, although for the latter we include the effect of the parameters M and R as explained in appendix C. This is not a serious defect, since for Sp$\bar{p}$S and Tevatron energies the neglected subprocesses do not contribute too much. The second reason was already mentioned below eq. (3.2). In the existing parametrizations for the parton distribution functions one never distinguishes between M and R, although the second order anomalous dimension depends on the operator renormalization (= mass factorization) as well as the coupling constant renormalization. Therefore, changing R in the $O(\alpha_s)$-corrected DY correction term has to be solely compensated by the $O(\alpha_s^2)$ corrections. Bearing these remarks in mind we can proceed with the discussion of the tables.

In tables 5–8 both scales are taken in the regions: $\frac{1}{2}M_Z \leqslant M, R \leqslant 2M_Z$. At $\sqrt{S} = 0.63$ TeV we observe an improvement in the stability of the cross section (or

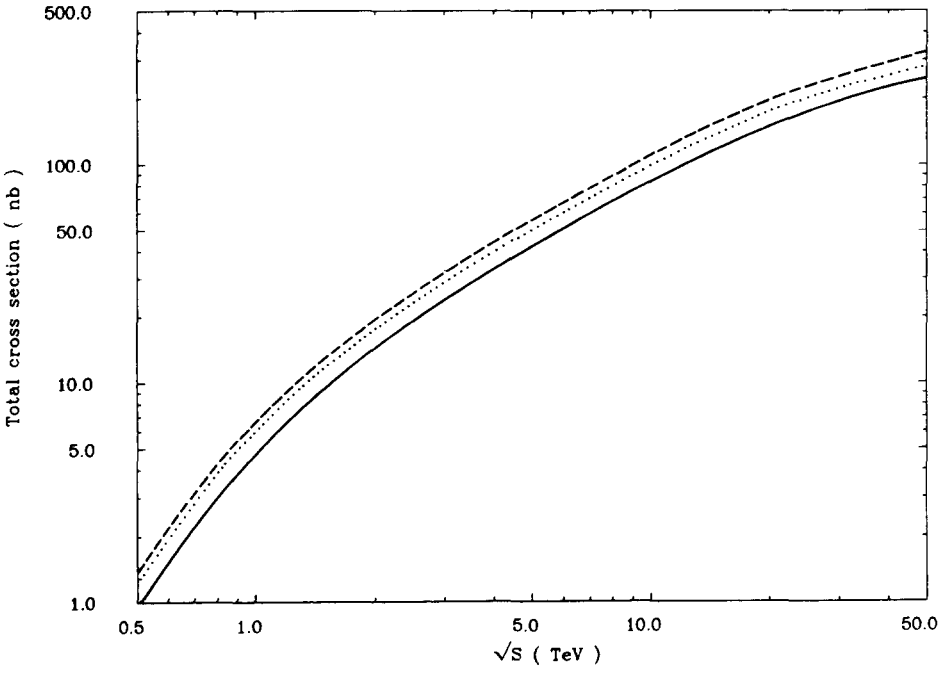

Fig. 11. The total cross section for the $W^+ + W^-$ production at a pp-collider in three approximations. Solid line: Born; dotted line: $O(\alpha_s)$ corrected; dashed line: $O(\alpha_s^2)$ corrected.

TABLE 1
The total cross section for Z-production in three approximations at SpS̄, Tevatron, LHC and SSC. The value between brackets is the sum of the contributions from $\Delta_{q\bar{q}}^{(1),H}$ and $\Delta_{qg}^{(1)}$.

		Z production rate (nb)		
	$\sqrt{S}$ (TeV)	DO1	EHLQ	DFLM4
Born	0.63	1.37	1.37	1.36
$O(\alpha_s)$		1.78 (−0.08)	1.79 (−0.08)	1.79 (−0.07)
$O(\alpha_s^2)$		1.95	1.95	1.96
Born	1.8	4.71	4.55	4.93
$O(\alpha_s)$		5.85 (−0.53)	5.64 (−0.52)	6.16 (−0.52)
$O(\alpha_s^2)$		6.45	6.22	6.78
Born	16.0	40.8	32.4	39.9
$O(\alpha_s)$		46.3 (−9.0)	37.0 (−6.9)	46.7 (−7.4)
$O(\alpha_s^2)$		52.3	41.8	52.5
Born	40.0	100.0	71.1	76.1
$O(\alpha_s)$		108.0 (−28.0)	79.0 (−17.0)	86.2 (−17.0)
$O(\alpha_s^2)$		124.0	90.6	98.3

TABLE 2
The total cross section for $W^+ + W^-$ production in three approximations at $Sp\bar{p}S$, Tevatron, LHC and SSC. The value between brackets is the sum of the contributions from $\Delta_{q\bar{q}}^{(1),H}$ and $\Delta_{qg}^{(1)}$.

	$\sqrt{S}$ (TeV)	$W^+ + W^-$ production rate (nb)		
		DO1	EHLQ	DFLM4
Born	0.63	4.69	4.16	4.39
$O(\alpha_s)$		6.11 (−0.31)	5.42 (−0.28)	5.76 (−0.26)
$O(\alpha_s^2)$		6.70	5.95	6.33
Born	1.8	15.4	14.5	16.3
$O(\alpha_s)$		19.0 (−1.9)	17.9 (−1.9)	20.3 (−1.9)
$O(\alpha_s^2)$		21.1	19.8	22.4
Born	16.0	127.0	100.0	131.0
$O(\alpha_s)$		141.0 (−31.0)	123.0 (−23.0)	153.0 (−25.0)
$O(\alpha_s^2)$		161.0	128.0	173.0
Born	40.0	300.0	213.0	232.0
$O(\alpha_s)$		313.0 (−95.0)	233.0 (−56.0)	262.0 (−53.0)
$O(\alpha_s^2)$		362.0	269.0	300.0

TABLE 3
σ_ZBR and $\sigma_{W^+ + W^-}$BR for CERN. We have used $BR(Z \to e^+e^-) = 3.35 \times 10^{-2}$ and $BR(W \to e\nu) = 0.109$ (see refs. [18] and [19]).

	$\sqrt{S} = 0.63$ TeV			
	DO1	EHLQ	DFLM4	UA2 [16]
	$\sigma_Z \times BR(Z \to e^+e^-)$ (pb)			
Born	45.8	45.9	45.7	
$O(\alpha_s)$	59.8	59.9	60.0	$70.4 \pm 5.5 \pm 4.0$
$O(\alpha_s^2)$	65.4	65.5	65.6	
	$\sigma_{W^+ + W^-} \times BR(W \to e\nu)$ (pb)			
Born	511	453	479	
$O(\alpha_s)$	666	590	628	$660 \pm 15 \pm 37$
$O(\alpha_s^2)$	731	649	690	

more precisely S_n) under changes of M and R, while going from the Born to the $O(\alpha_s^2)$ level. The same applies to the results for $\sqrt{S} = 1.8$ TeV, although the difference between S_1 and S_2 is hardly noticeable. What is very striking is that there is almost no difference between S_0 (Born) on the one hand and S_1, S_2 on the other hand. At $\sqrt{S} = 16$ and 40 TeV the result for S_1 is much more stable than for S_0, but for S_2 the stability diminishes compared to S_1. The latter is probably due to the fact that we have not included the mass factorization and renormalization

TABLE 4
σ_ZBR and $\sigma_{W^+ + W^-}$BR for Tevatron. We have used BR($Z \to e^+e^-$) = 3.35×10^{-2} and BR($W \to e\nu$) = 0.109 (see refs. [18] and [19]).

	$\sqrt{S}$ = 1.8 TeV			
	DO1	EHLQ	DFLM4	CDF [17]
	$\sigma_Z \times$ BR($Z \to e^+e^-$) (nb)			
Born	0.158	0.152	0.165	
$O(\alpha_s)$	0.196	0.189	0.206	$0.197 \pm 0.012 \pm 0.032$
$O(\alpha_s^2)$	0.216	0.208	0.227	
	$\sigma_{W^+ + W^-} \times$ BR($W \to e\nu$) (nb)			
Born	1.68	1.58	1.77	
$O(\alpha_s)$	2.08	1.95	2.21	$2.06 \pm 0.04 \pm 0.34$
$O(\alpha_s^2)$	2.30	2.16	2.44	

TABLE 5
The functions S_0, S_1 and S_2 (first, second and third row, respectively) for Z-production at Sp$\bar{p}$S ($\sqrt{S}$ = 0.63 TeV). The variables M and R are the factorization and renormalization scales.

	R/M_Z				
M/M_Z	$\frac{1}{2}$	$\frac{1}{2}\sqrt{2}$	1	$\sqrt{2}$	2
$\frac{1}{2}$	1.09	1.09	1.09	1.09	1.09
	1.05	1.04	1.03	1.02	1.01
	1.02	1.01	1.01	1.00	0.99
$\frac{1}{2}\sqrt{2}$	1.04	1.04	1.04	1.04	1.04
	1.04	1.03	1.01	1.00	0.99
	1.02	1.01	1.00	1.00	0.99
1	1.00	1.00	1.00	1.00	1.00
	1.03	1.01	1.00	0.99	0.98
	1.02	1.01	1.00	0.99	0.98
$\sqrt{2}$	0.96	0.96	0.96	0.96	0.96
	1.02	1.01	0.99	0.98	0.97
	1.02	1.01	1.00	0.99	0.98
2	0.93	0.93	0.93	0.93	0.93
	1.02	1.00	0.98	0.97	0.96
	1.02	1.01	1.00	0.99	0.98

TABLE 6
The functions S_0, S_1 and S_2 (first, second and third row, respectively) for Z-production at Tevatron ($\sqrt{S}$ = 1.8 TeV). The variables M and R are the factorization and renormalization scales.

	R/M_Z				
M/M_Z	$\frac{1}{2}$	$\frac{1}{2}\sqrt{2}$	1	$\sqrt{2}$	2
$\frac{1}{2}$	0.99	0.99	0.99	0.99	0.99
	1.02	1.01	1.00	0.99	0.98
	1.00	0.99	0.98	0.97	0.97
$\frac{1}{2}\sqrt{2}$	1.00	1.00	1.00	1.00	1.00
	1.02	1.01	1.00	0.99	0.98
	1.01	1.00	0.99	0.98	0.97
1	1.00	1.00	1.00	1.00	1.00
	1.02	1.01	1.00	0.99	0.98
	1.02	1.01	1.00	0.99	0.98
$\sqrt{2}$	1.00	1.00	1.00	1.00	1.00
	1.03	1.01	1.00	0.99	0.98
	1.03	1.02	1.01	1.00	0.99
2	1.00	1.00	1.00	1.00	1.00
	1.03	1.02	1.01	1.00	0.99
	1.04	1.03	1.02	1.01	1.01

terms from $\Delta_{qg}^{(2)}$. This shows once more that for LHC and SSC the $O(\alpha_s^2)$ contribution from the qg-subprocess will not be negligible. However, it is also possible that at very small x-values the parametrization of the parton distribution function does not exactly reproduce the M-evolution. From the tables we infer that at fixed M the function S_n ($n \geqslant 1$) decreases for increasing R. For fixed R the behaviour of S_n depends on the energy that one is considering. At $\sqrt{S}$ = 0.63 TeV S_1 decreases, whereas S_2 nearly remains constant, when M gets larger. For Tevatron S_1 remains almost constant, whereas S_2 increases. At $\sqrt{S}$ = 16 and 40 TeV both quantities increase for growing M. Moreover, there is a large variation in S_2, if M is varied between $\frac{1}{2}M_Z$ and $2M_Z$. The dependence on R is less pronounced. Putting $M = R$ we see that S_n grows when both parameters increase. Therefore, we do not see any minimum in S_n contrary to what has been observed in DY production at fixed target energies (e.g. $\sqrt{S}$ = 27.4 GeV, see ref. [22]). The PMS scheme [23] does not seem to work here.

Summarizing our results we conclude that the contribution of the gluon–gluon process (3.7) to the DY cross section is very small. This also applies to the singlet part of the $q\bar{q}$ (3.4d) and the qq (3.8) reactions. This statement even holds at very large energy, where these contributions never exceed the 1% level. The minor role of the gluon–gluon fusion in the DY process contrasts with that observed in other

TABLE 7
The functions S_0, S_1 and S_2 (first, second and third row, respectively) for Z-production at LHC ($\sqrt{S}$ = 16.0 TeV). The variables M and R are the factorization and renormalization scales.

	R/M_Z				
M/M_Z	$\frac{1}{2}$	$\frac{1}{2}\sqrt{2}$	1	$\sqrt{2}$	2
$\frac{1}{2}$	0.83	0.83	0.83	0.83	0.83
	0.96	0.94	0.93	0.92	0.91
	0.94	0.92	0.91	0.90	0.89
$\frac{1}{2}\sqrt{2}$	0.91	0.91	0.91	0.91	0.91
	0.99	0.98	0.97	0.96	0.95
	0.97	0.96	0.95	0.95	0.94
1	1.00	1.00	1.00	1.00	1.00
	1.02	1.01	1.00	0.99	0.99
	1.01	1.01	1.00	0.99	0.99
$\sqrt{2}$	1.08	1.08	1.08	1.08	1.08
	1.03	1.03	1.02	1.02	1.01
	1.05	1.05	1.04	1.04	1.03
2	1.16	1.16	1.16	1.16	1.16
	1.04	1.04	1.04	1.04	1.03
	1.09	1.09	1.08	1.08	1.08

processes like heavy flavour production [21]. This implies that besides the gluon flux, the behaviour of the Wilson coefficient is of utmost importance in determining the size of the higher order radiative corrections. Furthermore, we have shown that the reliability of the parton distribution functions becomes much less if one makes predictions for cross sections at energies much larger than 1.8 TeV. This is also corroborated by the sensitivity of the cross section to the mass factorization and renormalization scales at very large energies, such as for LHC and SSC. Finally, we observe that the missing parts given by $\Delta_{qg}^{(2)}$ and $\Delta_{q\bar{q}}^{(2),H}$ are not completely negligible and therefore have to be calculated too. This will be done in the near future, so that the complete $O(\alpha_s^2)$-correction to the DY K-factor will be known.

Appendix A

THE PHASE-SPACE INTEGRALS

A large part of the calculation of the gg-contribution to the Drell–Yan correction term consists of performing three particle phase space integrations. Here we will discuss some of the details of these computations and also will give some useful results.

TABLE 8
The functions S_0, S_1 and S_2 (first, second and third row, respectively) for Z-production at SSC ($\sqrt{S} = 40.0$ TeV). The variables M and R are the factorization and renormalization scales.

M/M_Z	R/M_Z				
	$\frac{1}{2}$	$\frac{1}{2}\sqrt{2}$	1	$\sqrt{2}$	2
$\frac{1}{2}$	0.77	0.77	0.77	0.77	0.77
	0.95	0.94	0.93	0.92	0.90
	0.93	0.92	0.90	0.89	0.88
$\frac{1}{2}\sqrt{2}$	0.88	0.88	0.88	0.88	0.88
	0.99	0.98	0.97	0.96	0.95
	0.98	0.96	0.95	0.94	0.93
1	1.00	1.00	1.00	1.00	1.00
	1.01	1.01	1.00	0.99	0.99
	1.02	1.01	1.00	0.99	0.99
$\sqrt{2}$	1.12	1.12	1.12	1.12	1.12
	1.02	1.02	1.01	1.01	1.01
	1.05	1.05	1.04	1.04	1.03
2	1.23	1.23	1.23	1.23	1.23
	1.01	1.01	1.02	1.02	1.02
	1.09	1.09	1.09	1.08	1.08

For the subprocess

$$g(k_1) + g(k_2) \to V(q) + q(p_1) + \bar{q}(p_2) \tag{A.1}$$

the three particle phase space integral is defined by

$$\int d\,PS^{(3)} = \frac{1}{(2\pi)^{2n-3}} \int d^n q \int d^n p_1 \int d^n p_2\, \delta^+(q^2 - Q^2)\delta^+(p_1^2)\delta^+(p_2^2)$$
$$\times \delta^n(k_1 + k_2 - q - p_1 - p_2)\,. \tag{A.2}$$

In the c.m. of the incoming gluons it can be parametrized as

$$\int d\,PS^{(3)} = \frac{1}{(4\pi)^n} \frac{s^{1-n/2}}{\Gamma(n-3)} \int_0^\pi d\theta \int_0^\pi d\phi (\sin\theta)^{n-3} (\sin\phi)^{n-4}$$
$$\times \int_{Q^2}^{s} ds_1 \int_{sQ^2/s_1}^{s+Q^2-s_1} ds_2 \left\{(s_1 s_2 - sQ^2)(s + Q^2 - s_1 - s_2)\right\}^{n/2-2} \tag{A.3}$$

with $s=(k_1+k_2)^2$, $s_1=(p_1+q)^2$ and $s_2=(p_2+q)^2$. Furthermore, in this frame the momenta are given by [24]

$$k_1=\tfrac{1}{2}\sqrt{s}\,(1,0,\ldots,0,0,1)\,,\qquad k_2=\tfrac{1}{2}\sqrt{s}\,(1,0,\ldots,0,0,-1)\,,$$

$$p_1=\frac{s-s_2}{2\sqrt{s}}(1,0,\ldots,0,\sin\theta,\cos\theta)\,,$$

$$p_2=\frac{s-s_1}{2\sqrt{s}}(1,0,\ldots,\sin\chi\sin\phi,\cos\chi\sin\theta+\sin\chi\cos\phi\cos\theta,$$

$$\cos\chi\cos\theta-\sin\chi\cos\phi\sin\theta)\,, \qquad \text{(A.4)}$$

where χ is the angle between the momenta p_1 and p_2. It satisfies the relation

$$\sin^2(\tfrac{1}{2}\chi)=\frac{s(s+Q^2-s_1-s_2)}{(s-s_1)(s-s_2)}\,. \qquad \text{(A.5)}$$

For the actual calculations we rewrite eq. (A.3) as

$$\int \mathrm{d}\,\mathrm{PS}_3^{\mathrm{DY}}=\frac{1}{(4\pi)^n}\frac{(Q^2)^{n-3}}{\Gamma(n-3)}x^{3-n}(1-x)^{2n-5}\int_0^{\pi}\mathrm{d}\theta\int_0^{\pi}\mathrm{d}\phi(\sin\theta)^{n-3}(\sin\phi)^{n-4}$$

$$\times\int_0^1\mathrm{d}y\int_0^1\mathrm{d}z\{z(1-z)\}^{n/2-2}\{y(1-y)\}^{n-3}\{1-(1-x)y\}^{1-n/2}. \qquad \text{(A.6)}$$

The variables x, y and z are defined by

$$x=Q^2/s\,,\qquad s_1=s\{1-(1-x)y\}\,,$$

$$s_2=s\frac{\{x+(1-x)^2y(1-y)(1-z)\}}{1-(1-x)y}\,. \qquad \text{(A.7)}$$

Before giving the results, let us fix the notation. We express the matrix element in terms of the invariants

$$P_{ij}=(l_i+l_j)^2\,,\qquad B_1=P_{13}+P_{14}\,,\qquad B_2=P_{23}+P_{24} \qquad \text{(A.8)}$$

with $l_1=p_1$, $l_2=p_2$, $l_3=-k_1$, $l_4=-k_2$ and $l_5=q$. The last two invariants appear

after partional fractioning, i.e.

$$\frac{1}{P_{13}P_{14}} = \frac{1}{B_1}\left\{\frac{1}{P_{13}} + \frac{1}{P_{14}}\right\}, \tag{A.9}$$

$$\frac{1}{P_{23}P_{24}} = \frac{1}{B_2}\left\{\frac{1}{P_{23}} + \frac{1}{P_{24}}\right\} \tag{A.10}$$

which is needed to handle the angular integrals. After this partional fractioning all the angular integrations can be performed using

$$\int_0^\pi \mathrm{d}\theta \int_0^\pi \mathrm{d}\phi \, \frac{(\sin\theta)^{n-3}(\sin\phi)^{n-4}}{(1-\cos\theta)^i(1-\cos\alpha\cos\theta-\sin\alpha\cos\phi\sin\theta)^j}$$

$$= 2^{1-i-j}\pi \frac{\Gamma(\frac{1}{2}n-1-j)\Gamma(\frac{1}{2}n-1-i)}{\Gamma(n-2-i-j)} \frac{\Gamma(n-3)}{\Gamma^2(\frac{1}{2}n-1)} F\left(i,j;\tfrac{1}{2}n-1;\cos^2\tfrac{1}{2}\alpha\right), \tag{A.11}$$

where Γ is the gamma function and $F(a,b;c;x)$ denotes the hypergeometric function.

To perform the remaining integrations over y and z, the following set of integrals turned out to be very useful.

$$\int_0^1 \mathrm{d}z z^\tau (1-z)^{\gamma-1} F\left(\alpha,\beta;\gamma;-\frac{(1-z)}{z}w\right)$$

$$= w^{1+\tau}\frac{\Gamma(\gamma)\Gamma(1+\alpha+\tau)\Gamma(1+\beta+\tau)}{\Gamma(1+\gamma+\tau)\Gamma(1+\alpha+\beta+\tau)}$$

$$\times F(1+\alpha+\tau,1+\beta+\tau;1+\alpha+\beta+\tau;1-w). \tag{A.12}$$

Furthermore, defining

$$I(i,j) = \int_0^1 \mathrm{d}y \, \frac{y^{i+\varepsilon}(1-y)^{\varepsilon}}{\{1-(1-x)y\}^{j}} F\left(\tfrac{1}{2}\varepsilon, \varepsilon; 1+\varepsilon; (1-x)y\right), \tag{A.13}$$

$$J(i,j) = \int_0^1 \mathrm{d}y y^{i+\varepsilon}(1-y)^{\varepsilon}\{1-(1-x)y\}^{-j-\varepsilon/2} \tag{A.14}$$

we find

$$I(-1,0) = 1/\varepsilon - \varepsilon\zeta(2) + \varepsilon^2\left(2\zeta(3) + \tfrac{1}{2}\mathrm{Li}_3(1-x)\right), \tag{A.15}$$

$$I(0,0) = 1 - 2\varepsilon + \varepsilon^2\left[\tfrac{1}{2}\mathrm{Li}_2(1-x) - \zeta(2) - \frac{1}{2}\frac{x\ln x}{(1-x)} + \tfrac{7}{2}\right], \tag{A.16}$$

$$I(1,0) = \tfrac{1}{2} - \varepsilon + \varepsilon^2\left[\tfrac{1}{4}\mathrm{Li}_2(1-x) - \tfrac{1}{2}\zeta(2) + \frac{1}{8}\frac{(x^2-2x)}{(1-x)^2}\ln x + \frac{1}{16}\frac{(29-31x)}{(1-x)}\right], \tag{A.17}$$

$$I(0,1) = \frac{1}{(1-x)}\left\{-\ln x + \varepsilon\left[-2\mathrm{Li}_2(1-x) - \tfrac{1}{2}\ln^2 x\right]\right.$$
$$\left. + \varepsilon^2\left[-3S_{1,2}(1-x) + 4\mathrm{Li}_3(1-x) - \tfrac{5}{2}\ln x\,\mathrm{Li}_2(1-x) + \zeta(2)\ln x - \tfrac{1}{6}\ln^3 x\right]\right\}, \tag{A.18}$$

$$I(0,2) = \frac{1}{x(1-x)}\left\{(1-x) + \varepsilon(1+x)\ln x\right.$$
$$\left. + \varepsilon^2\left[\tfrac{1}{2}(5+3x)\mathrm{Li}_2(1-x) - (1-x)\zeta(2) + \tfrac{1}{4}(2+x)\ln^2 x\right]\right\}, \tag{A.19}$$

$$I(0,3) = \frac{1}{x^2(1-x)}\left\{\tfrac{1}{2}(1-x^2) + \varepsilon\left[\tfrac{1}{2}(1+x^2)\ln x - \tfrac{1}{2}(1-x^2)\right]\right.$$
$$+ \varepsilon^2\left[\tfrac{1}{4}(5+3x^2)\mathrm{Li}_2(1-x) - \tfrac{1}{2}(1-x^2)\zeta(2) + \tfrac{1}{8}(2+x^2)\ln^2 x\right.$$
$$\left.\left. - \tfrac{1}{4}(2+3x+2x^2)\ln x + \tfrac{1}{4}x(1-x)\right]\right\}. \tag{A.20}$$

For the integrals J we have

$$J(-1,0) = 1/\varepsilon + \varepsilon\left[\tfrac{1}{2}\,\mathrm{Li}_2(1-x) - \zeta(2)\right] + \varepsilon^2\left[2\zeta(3) - \tfrac{1}{4}S_{1,2}(1-x) - \mathrm{Li}_3(1-x)\right], \tag{A.21}$$

$$J(0,0) = \frac{1}{(1-x)}\Big\{(1-x) + \varepsilon\left[\tfrac{1}{2}x\ln x - \tfrac{3}{2}(1-x)\right] + \varepsilon^2\left[\tfrac{1}{2}(1+x)\mathrm{Li}_2(1-x)\right.$$
$$\left. -(1-x)\zeta(2) + \tfrac{1}{8}x\ln^2 x - \tfrac{3}{4}x\ln x + \tfrac{9}{4}(1-x)\right]\Big\}, \tag{A.22}$$

$$J(1,0) = \frac{1}{(1-x)^2}\Big\{\tfrac{1}{2}(1-x)^2 + \varepsilon\left[-\tfrac{1}{4}(x^2-2x)\ln x - \tfrac{1}{8}(5-7x)(1-x)\right]$$
$$+\varepsilon^2\left[\tfrac{1}{4}(1+2x-x^2)\mathrm{Li}_2(1-x) - \tfrac{1}{2}(1-x)^2\zeta(2)\right.$$
$$\left. -\tfrac{1}{16}(x^2-2x)\ln^2 x + \tfrac{1}{16}(7x^2-8x)\ln x + \tfrac{1}{32}(27-45x)(1-x)\right]\Big\}, \tag{A.23}$$

$$J(0,1) = \frac{1}{(1-x)}\Big\{-\ln x + \varepsilon\left[-2\,\mathrm{Li}_2(1-x) - \tfrac{1}{4}\ln^2 x\right] + \varepsilon^2\left[4\,\mathrm{Li}_3(1-x)\right.$$
$$\left. -2S_{1,2}(1-x) - \tfrac{3}{2}\ln x\,\mathrm{Li}_2(1-x) + \zeta(2)\ln x - \tfrac{1}{24}\ln^3 x\right]\Big\}, \tag{A.24}$$

$$J(0,2) = \frac{1}{x(1-x)}\Big\{(1-x) + \varepsilon\left[\tfrac{1}{2}(1+2x)\ln x - \tfrac{1}{2}(1-x)\right]$$
$$+\varepsilon^2\left[\tfrac{3}{2}(1+x)\mathrm{Li}_2(1-x) - (1-x)\zeta(2) + \tfrac{1}{8}(1+2x)\ln^2 x\right.$$
$$\left. -\tfrac{1}{4}(1+2x)\ln x + \tfrac{1}{4}(1-x)\right]\Big\}, \tag{A.25}$$

$$J(0,3) = \frac{1}{x^2(1-x)}\Big\{\tfrac{1}{2}(1-x^2) + \varepsilon\left[\tfrac{1}{4}(1+2x^2)\ln x - \tfrac{5}{8}(1-x^2)\right]$$
$$+\varepsilon^2\left[\tfrac{3}{4}(1+x^2)\mathrm{Li}_2(1-x) - \tfrac{1}{2}(1-x^2)\zeta(2) + \tfrac{1}{16}(1+2x^2)\ln^2 x\right.$$
$$\left. -\tfrac{1}{16}(5+12x+10x^2)\ln x + \tfrac{13}{32}(1-x^2)\right]\Big\}. \tag{A.26}$$

Using the integrals listed above and some properties of the hypergeometric function [25], we were able to solve most of the 61 phase space integrals for the gg-subprocess. However, we also encountered some integrals which had to be computed using brute force methods. The results of the latter will be given

subsequently. In the following list we have left out an overall factor

$$\frac{\pi}{(4\pi)^4}\left(\frac{Q^2}{4\pi\mu^2}\right)^{\varepsilon}\frac{\Gamma^2(1+\frac{1}{2}\varepsilon)}{\Gamma^2(1+\varepsilon)}x^{-\varepsilon}(1-x)^{2\varepsilon}. \tag{A.27}$$

List of gg phase-space integrals
"propagators" $\to \int \mathrm{d}\,\mathrm{PS}^{(3)}$ "propagators"

$$\frac{s^3}{B_1B_2P_{13}P_{23}} = \frac{16}{\varepsilon^3}\frac{1}{(1-x)}\{1+\varepsilon^2[\tfrac{1}{2}\,\mathrm{Li}_2(1-x)-\zeta(2)]$$
$$+\varepsilon^3[-\tfrac{1}{4}S_{1,2}(1-x)-\tfrac{3}{4}\,\mathrm{Li}_3(1-x)+2\zeta(3)]\}, \tag{A.28}$$

$$\frac{s^3}{B_1B_2P_{13}P_{24}} = \frac{16}{\varepsilon^3}\frac{1}{(1-x)}\{1-\tfrac{1}{2}\varepsilon\ln x+\varepsilon^2[-\tfrac{1}{2}\,\mathrm{Li}_2(1-x)-\zeta(2)-\tfrac{1}{4}\ln^2 x]$$
$$+\varepsilon^3[2\zeta(3)-2S_{1,2}(1-x)+\tfrac{3}{4}\,\mathrm{Li}_3(1-x)+\tfrac{1}{2}\zeta(2)\ln x$$
$$-\tfrac{5}{4}\ln x\,\mathrm{Li}_2(1-x)-\tfrac{1}{12}\ln^3 x]\}, \tag{A.29}$$

$$\frac{s^3}{P_{13}P_{15}P_{23}P_{25}} = \frac{8}{\varepsilon^2}\frac{1}{(1+x)}\Bigg\{-2\ln x+\varepsilon[-4\,\mathrm{Li}_2(1-x)-2\,\mathrm{Li}_2(-x)-\zeta(2)$$
$$+\tfrac{1}{2}\ln^2 x-2\ln x\ln(1+x)]$$
$$+\varepsilon^2\Bigg[2S_{1,2}(-x)+4\,\mathrm{Li}_3(1-x)-3\,\mathrm{Li}_3(-x)+4\,\mathrm{Li}_3\left(\frac{1-x}{1+x}\right)$$
$$-4\,\mathrm{Li}_3\left(-\frac{1-x}{1+x}\right)-\tfrac{5}{2}\zeta(3)+\ln x\,\mathrm{Li}_2(1-x)+2\ln x\,\mathrm{Li}_2(-x)$$
$$+2\ln(1+x)\mathrm{Li}_2(-x)+\tfrac{3}{2}\zeta(2)\ln x+\zeta(2)\ln(1+x)+\tfrac{1}{3}\ln^3 x$$
$$+\tfrac{1}{2}\ln^2 x\ln(1+x)+\ln x\ln^2(1+x)\Bigg]\Bigg\}, \tag{A.30}$$

$$\frac{s^3}{P_{13}P_{15}P_{24}P_{25}} = \frac{8}{\varepsilon^2}\frac{1}{x}\{-\ln x+\varepsilon[-2\,\mathrm{Li}_2(1-x)+2\,\mathrm{Li}_2(-x)$$
$$+\zeta(2)-\ln^2 x+2\ln x\ln(1+x)]$$

$$+\varepsilon^2\Big[-5S_{1,2}(1-x)-3S_{1,2}(-x)+8\,\mathrm{Li}_3(1-x)+\tfrac{7}{2}\,\mathrm{Li}_3(-x)$$

$$-4\,\mathrm{Li}_3\left(\frac{1-x}{1+x}\right)+4\,\mathrm{Li}_3\left(-\frac{1-x}{1+x}\right)+3\zeta(3)-\tfrac{9}{2}\ln x\,\mathrm{Li}_2(1-x)$$

$$-\tfrac{3}{2}\ln x\,\mathrm{Li}_2(-x)-3\ln(1+x)\,\mathrm{Li}_2(-x)-\tfrac{3}{2}\zeta(2)\ln(1+x)$$

$$+2\zeta(2)\ln x-\tfrac{1}{2}\ln^3 x+\tfrac{1}{4}\ln^2 x\ln(1+x)-\tfrac{3}{2}\ln x\ln^2(1+x)\Big] \quad \text{(A.31)}$$

$$\frac{s^2}{P_{15}P_{23}P_{25}}=-\frac{8}{\varepsilon}\Big\{-\mathrm{Li}_2(-x)-\tfrac{1}{2}\zeta(2)+\tfrac{1}{2}\ln^2 x-\ln x\ln(1+x)$$

$$+\varepsilon\Big[2S_{1,2}(1-x)+\tfrac{3}{2}S_{1,2}(-x)-2\,\mathrm{Li}_3(1-x)-\tfrac{3}{4}\,\mathrm{Li}_3(-x)$$

$$+2\,\mathrm{Li}_3\left(\frac{1-x}{1+x}\right)-2\,\mathrm{Li}_3\left(-\frac{1-x}{1+x}\right)-\tfrac{3}{4}\zeta(3)+2\ln x\,\mathrm{Li}_2(1-x)$$

$$+\tfrac{1}{4}\ln x\,\mathrm{Li}_2(-x)+\tfrac{3}{2}\ln(1+x)\,\mathrm{Li}_2(-x)-\tfrac{1}{4}\zeta(2)\ln x+\tfrac{3}{4}\zeta(2)\ln(1+x)$$

$$+\tfrac{5}{24}\ln^3 x-\tfrac{1}{8}\ln^2 x\ln(1+x)+\tfrac{3}{4}\ln x\ln^2(1+x)\Big]\Big\}, \quad \text{(A.32)}$$

$$\frac{sP_{14}}{P_{15}P_{23}P_{25}}=x\left(\frac{s^2}{P_{15}P_{23}P_{25}}\right)+\frac{4}{\varepsilon}\Big\{-\ln x-(1-x)$$

$$+\varepsilon\Big[-(1+2x)\big(\mathrm{Li}_2(-x)+\tfrac{1}{2}\zeta(2)+\ln x\ln(1+x)\big)$$

$$-2\,\mathrm{Li}_2(1-x)+x\ln^2 x+\tfrac{1}{2}(3-2x)\ln x+\tfrac{5}{2}(1-x)\Big]\Big\}, \quad \text{(A.33)}$$

$$\frac{P_{14}^2}{P_{15}P_{23}P_{25}}=x^2\left(\frac{s^2}{P_{15}P_{23}P_{25}}\right)-\frac{4}{\varepsilon}\Big\{\tfrac{1}{2}(2x-1)\ln x-\tfrac{1}{4}(3-5x)(1-x)+\varepsilon\Big[(6x^2+2x-1)$$

$$\times\big(\tfrac{1}{2}\,\mathrm{Li}_2(-x)+\tfrac{1}{4}\zeta(2)+\tfrac{1}{2}\ln x\ln(1+x)\big)+(2x-1)\mathrm{Li}_2(1-x)-\tfrac{3}{2}x^2\ln^2 x$$

$$+\tfrac{1}{8}(10x^2-18x+7)\ln x+\tfrac{3}{16}(13-19x)(1-x)\Big]\Big\}. \quad \text{(A.34)}$$

Appendix B

THE STRUCTURE FUNCTIONS FOR qq, $\bar{q}\bar{q}$ AND $q\bar{q}$, SINGLET

In this appendix we will discuss the structure functions for the subprocesses

$$q+q\to V+q+q, \quad \text{(B.1)}$$

$$\bar{q}+\bar{q}\to V+\bar{q}+\bar{q}, \quad \text{(B.2)}$$

$$q+\bar{q}\to V+q+\bar{q},\text{singlet} \quad \text{(B.3)}$$

in some detail, because they are non-trivial due to the somewhat complicated structure of the Drell–Yan correction term.

The diagrams for the subprocesses under discussion are given in fig. 12. In case of non-identical quarks only the diagrams corresponding to the amplitudes A_1 and A_2 have to be taken into account. However, if identical quarks appear in the initial and/or final state, also the crossed diagrams contribute (amplitudes A_3 and A_4). Notice that each amplitude A_i is gauge invariant. In ref. [24] the Drell–Yan correction term has been computed for $V=\gamma^*$. The calculation was done by dividing the Drell–Yan correction term into four parts:

$$\begin{aligned}
&\Delta_{qq} \leftrightarrow |A_i|^2 ,\\
&\Delta_{qq}^{I} \leftrightarrow A_1 A_2^\dagger \quad \text{and} \quad A_3 A_4^\dagger ,\\
&\Delta_{qq}^{init} \leftrightarrow A_1 A_3^\dagger \quad \text{and} \quad A_2 A_4^\dagger ,\\
&\Delta_{qq}^{final} \leftrightarrow A_1 A_4^\dagger \quad \text{and} \quad A_2 A_3^\dagger .
\end{aligned} \tag{B.4}$$

They then found

$$\Delta_{qq}(x) = \left(\frac{\alpha_s}{4\pi}\right)^2 \frac{N^2-1}{N} \Sigma^{qq}(x) , \tag{B.5}$$

$$\Delta_{qq}^{I}(x) = \left(\frac{\alpha_s}{4\pi}\right)^2 \frac{N^2-1}{N} \Sigma_I^{qq}(x) , \tag{B.6}$$

$$\Delta_{qq}^{init}(x) = \left(\frac{\alpha_s}{4\pi}\right)^2 \frac{N^2-1}{N^2} \Sigma_{cr}^{(3)}(x) , \tag{B.7}$$

$$\Delta_{qq}^{final}(x) = \left(\frac{\alpha_s}{4\pi}\right)^2 \frac{N^2-1}{N^2} \left(\Sigma_{cr}^{(2)}(x) - \Sigma_{cr}^{(1)}(x)\ln(1-x) - \Omega_{cr}^{(2)}(x)\right), \tag{B.8}$$

where the expressions for Σ^{qq}, Σ_I^{qq}, $\Sigma_{cr}^{(i)}$ and $\Omega_{cr}^{(2)}$ can be found in eqs. (6.9), (3.27), (7.6) and (7.8) and appendix D of chapter III in ref. [24], respectively. Notice that in this reference contrary to ref. [9] the momentum sum rules have been imposed on the splitting function $\Gamma_{gq}^{(1)}$.

Introducing also axial couplings the results of ref. [24] have to be slightly adapted. Contrary to the other processes we studied, the axial part of the coupling contributes differently to $\Delta_{qq}^{I}(x)$ from the vector part. This is due to the particular trace structure of the $A_1 A_2^\dagger$ ($A_3 A_4^\dagger$) interference term. In this paper we have not yet included this new contribution. Notice, however, that this only affects the results for Z-production, as W-production has no contributions from $\Delta_{qq}^{I}(x)$.

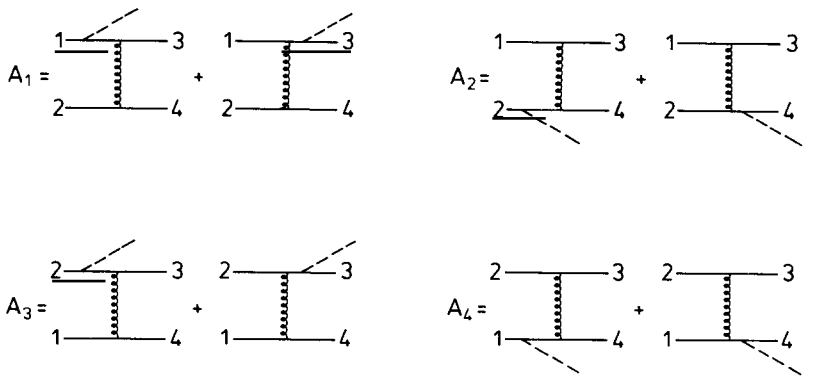

Fig. 12. The diagrams for the qq-subprocess. The amplitudes A_3 and A_4 only contribute in case of identical quarks in the initial and/or final state.

We will now give the structure functions for the above processes. Keeping in mind the correspondence between the Drell–Yan correction terms and the Feyman diagrams in fig. 12 (see eq. (B.4)), one finds for the qq and $\bar{q}\bar{q}$ contribution to the Z-production cross section

$$\frac{d\sigma^{qq+\bar{q}\bar{q}}}{dQ^2} = \tau\sigma_Z \int_0^1 dx \int_0^1 dx_1 \int_0^1 dx_2\, \delta(\tau - x x_1 x_2)\{Z_{qq}(x_1, x_2)\Delta_{qq}(x)$$

$$+ Z^{I}_{qq}(x_1, x_2)\Delta^{I}_{qq}(x) + Z^{id}_{qq}(x_1, x_2)\left(\Delta^{init}_{qq}(x) + \Delta^{final}_{qq}(x)\right)\}. \quad \text{(B.9)}$$

The structure functions Z_{qq} are given by

$$Z^{(I)}_{qq} = C^{(I)}_{u}(u_1 + c_1)(u_2 + c_2)$$

$$+ C^{(I)}_{ud}\{(u_1 + c_1)(d_2 + s_2) + (d_1 + s_1)(u_2 + c_2)\}$$

$$+ C^{(I)}_{d}(d_1 + s_1)(d_2 + s_2) + \{\text{quarks} \to \text{anti-quarks}\}, \quad \text{(B.10)}$$

$$Z^{id}_{qq} = C_u\{u_1 u_2 + c_1 c_2\} + C_d\{d_1 d_2 + s_1 s_2\}$$

$$+ \{\text{quarks} \to \text{anti-quarks}\} \quad \text{(B.11)}$$

with

$$C_u = 2\left(1 + \left(1 - \tfrac{8}{3}\sin^2\theta_W\right)^2\right), \tag{B.12}$$

$$C_d = 2\left(1 + \left(1 - \tfrac{4}{3}\sin^2\theta_W\right)^2\right), \tag{B.13}$$

$$C_{ud} = \tfrac{1}{2}(C_u + C_d), \tag{B.14}$$

$$C_u^I = 2\left(1 - \tfrac{8}{3}\sin^2\theta_W\right)^2, \tag{B.15}$$

$$C_d^I = 2\left(1 - \tfrac{4}{3}\sin^2\theta_W\right)^2, \tag{B.16}$$

$$C_{ud}^I = -2\left(1 - \tfrac{4}{3}\sin^2\theta_W\right)\left(1 - \tfrac{8}{3}\sin^2\theta_W\right). \tag{B.17}$$

Furthermore, u_i, d_i, s_i and c_i are the distribution functions for the up, down, strange and charm quarks for x_i, the barred quantities will represent the corresponding antiquarks. For the $q\bar{q}$-subprocess the cross section is given by

$$\frac{d\sigma^{q\bar{q}}}{dQ^2} = \tau\sigma_Z \int_0^1 dx \int_0^1 dx_1 \int_0^1 dx_2\, \delta(\tau - x x_1 x_2) \times \left\{Z_{q\bar{q}}(x_1, x_2)\Delta_{qq}(x) - Z_{q\bar{q}}^I(x_1, x_2)\Delta_{qq}^I(x)\right\} \tag{B.18}$$

with

$$\begin{aligned} Z_{q\bar{q}}^{(I)} = {} & C_u^{(I)}(u_1 + c_1)(\bar{u}_2 + \bar{c}_2) \\ & + C_{ud}^{(I)}\left\{(u_1 + c_1)(\bar{d}_2 + \bar{s}_2) + (d_1 + s_1)(\bar{u}_2 + \bar{c}_2)\right\} \\ & + C_d^{(I)}(d_1 + s_1)(\bar{d}_2 + \bar{s}_2) + \{1 \leftrightarrow 2\}. \end{aligned} \tag{B.19}$$

The corresponding formulae for W^--production are

$$\begin{aligned} \frac{d\sigma^{qq+\bar{q}\bar{q}}}{dQ^2} = {} & \tau\sigma_W \int_0^1 dx \int_0^1 dx_1 \int_0^1 dx_2\, \delta(\tau - x x_1 x_2)\left\{W_{qq}(x_1, x_2)\Delta_{qq}(x)\right. \\ & \left. + W_{qq}^{\text{init}}(x_1, x_2)\Delta_{qq}^{\text{init}}(x) + W_{qq}^{\text{final}}(x_1, x_2)\Delta_{qq}^{\text{final}}(x)\right\}, \end{aligned} \tag{B.20}$$

$$\frac{d\sigma^{q\bar{q}}}{dQ^2} = \tau\sigma_W \int_0^1 dx \int_0^1 dx_1 \int_0^1 dx_2\, \delta(\tau - x x_1 x_2) W_{q\bar{q}}(x_1, x_2)\Delta_{qq}(x) \tag{B.21}$$

with

$$W_{qq} = (\bar{u}_1 + \bar{c}_1)(\bar{d}_2 + \bar{s}_2) + (d_1 + s_1)(u_2 + c_2) + \{1 \leftrightarrow 2\}$$
$$+ 2(\bar{u}_1 + \bar{c}_1)(\bar{u}_2 + \bar{c}_2) + 2(d_1 + s_1)(d_2 + s_2), \tag{B.22}$$

$$W_{qq}^{\text{init}} = 2\{\bar{u}_1\bar{u}_2 + \bar{c}_1\bar{c}_2 + d_1d_2 + s_1s_2\}, \tag{B.23}$$

$$W_{qq}^{\text{final}} = \cos^2\theta_C\{\bar{u}_1\bar{d}_2 + \bar{c}_1\bar{s}_2 + d_1u_2 + s_1c_2\}$$
$$+ \sin^2\theta_C\{\bar{u}_1\bar{s}_2 + \bar{c}_1\bar{d}_2 + d_1c_2 + s_1u_2\} + \{1 \leftrightarrow 2\}, \tag{B.24}$$

$$W_{q\bar{q}} = (\bar{u}_1 + \bar{c}_1)(u_2 + c_2) + (d_1 + s_1)(\bar{d}_2 + \bar{s}_2) + \{1 \leftrightarrow 2\}$$
$$+ 2(\bar{u}_1 + \bar{c}_1)(d_2 + s_2) + 2(d_1 + s_1)(\bar{u}_2 + \bar{c}_2) \tag{B.25}$$

The cross sections for W^+ can be obtained by replacing all the quarks in the formulae for W^- production by anti-quarks and vice versa.

Appendix C

SCALE DEPENDENCE OF THE DRELL–YAN CORRECTION TERMS

When performing mass factorization in the DIS scheme one still has the freedom to choose arbitrary scales for the running coupling constant and the parton distribution functions. Mostly these scales are chosen to be equal to the invariant mass of the lepton pair (="natural" scale). In this appendix we will give the additional contributions to the Drell–Yan correction term when one no longer restricts oneself to the "natural" scales. Here we will only present the scale-dependent parts of the Drell–Yan correction term, the scale-independent pieces can be found elsewhere.

In the subsequent formulae we will use the shorthand notations

$$L_M = \ln\left(\frac{Q^2}{M^2}\right), \qquad L_R = \ln\left(\frac{Q^2}{R^2}\right), \tag{C.1}$$

where Q^2 is the invariant mass of the vector boson and M^2 and R^2 are the scales to be used in the parton distribution functions and the running coupling constant, respectively. Notice that for the "natural" scale we have $L_M = L_R = 0$, so that all the expressions given in this appendix are zero for this scale. Furthermore, we

introduce the distribution

$$\mathscr{D}_i(x) = \delta(1-x)\frac{\ln^{i+1}\delta}{(i+1)} + \theta(1-\delta-x)\frac{\ln^i(1-x)}{(1-x)}. \tag{C.2}$$

We will start with the scale-dependent contributions to the order α_s Drell–Yan correction terms. In the following we will omit overall factors $(\alpha_s/4\pi)^i$. For the $q\bar{q}$-subprocess we find

$$\Delta^{(1)}_{q\bar{q}}(x, Q^2, M^2, R^2) = C_F\{6\delta(1-x) + 8\mathscr{D}_0(x) - 4(1+x)\}L_M. \tag{C.3}$$

The additional term for the qg-process is given by

$$\Delta^{(1)}_{qg}(x, Q^2, M^2, R^2) = (1 - 2x + 2x^2)L_M. \tag{C.4}$$

In ref. [4] the second order $q\bar{q}$-subprocess has been calculated in the soft limit $x \to 1$. The scale-dependent part, however, can be determined exactly, because the second order non-singlet anomalous dimension has been calculated without the soft limit approximation (see ref. [26]). For numerical computations it is convenient to split the $q\bar{q}$ Drell–Yan correction term into a "soft + virtual" (S + V) and a "hard" (H) gluon piece, viz.

$$\Delta^{(2)}_{q\bar{q}}(x, Q^2, M^2, R^2) = \Delta^{(2),(S+V)}_{q\bar{q}}(x, Q^2, M^2, R^2) + \Delta^{(2),H}_{q\bar{q}}(x, Q^2, M^2, R^2) \tag{C.5}$$

with

$$\begin{aligned}
&\Delta^{(2),(S+V)}_{q\bar{q}}(x, Q^2, M^2, R^2) \\
&= \delta(1-x)\Big[C_F^2\{(18 - 32\zeta(2))L_M^2 + (15 + 24\zeta(2) + 112\zeta(3))L_M\} \\
&\quad + C_A C_F\{11L_M^2 - 22L_M L_R + (\tfrac{215}{3} + \tfrac{176}{3}\zeta(2) - 24\zeta(3))L_M - (\tfrac{22}{3} + \tfrac{176}{3}\zeta(2))L_R\} \\
&\quad + n_f C_F\{-2L_M^2 + 4L_M L_R - (\tfrac{38}{3} + \tfrac{32}{3}\zeta(2))L_M + (\tfrac{4}{3} + \tfrac{32}{3}\zeta(2))L_R\}\Big] \\
&\quad + C_F^2\big[96L_M\mathscr{D}_2(x) + (64L_M^2 + 144L_M)\mathscr{D}_1(x) \\
&\quad + (48L_M^2 + (52 + 64\zeta(2))L_M)\mathscr{D}_0(x)\big] \\
&\quad + C_A C_F\big[-\tfrac{88}{3}(L_M + L_R)\mathscr{D}_1(x) + (\tfrac{44}{3}L_M^2 - \tfrac{88}{3}L_M L_R \\
&\quad + (\tfrac{734}{9} - 16\zeta(2))L_M - 22L_R)\mathscr{D}_0(x)\big] \\
&\quad + n_f C_F\big[\tfrac{16}{3}(L_M + L_R)\mathscr{D}_1(x) + (-\tfrac{8}{3}L_M^2 + \tfrac{16}{3}L_M L_R - \tfrac{116}{9}L_M + 4L_R)\mathscr{D}_0(x)\big]
\end{aligned} \tag{C.6}$$

and

$$
\begin{aligned}
&\Delta_{q\bar{q}}^{(2),H}(x,Q^2,M^2,R^2)\\
&= C_F^2\Bigg\{\Bigg[-32\frac{\ln x}{(1-x)} - 32(1+x)\ln(1-x) + 24(1+x)\ln x - 40 - 8x\Bigg]L_M^2\\
&\quad + \Bigg[-16(1+x)\{\mathrm{Li}_2(x) + \zeta(2) + 3\ln^2(1-x) + \tfrac{1}{4}\ln^2 x - 3\ln x\ln(1-x)\}\\
&\quad -96\frac{\ln x\ln(1-x)}{(1-x)} - 72\frac{\ln x}{(1-x)} - (176+80x)\ln(1-x)\\
&\quad + (72+24x)\ln x - 112 - 24x\Bigg]L_M\Bigg\} + C_A C_F\Bigg\{-\tfrac{22}{3}(1+x)L_M^2 + \tfrac{44}{3}(1+x)L_M L_R\\
&\quad + \Bigg[(1+x)\{8\zeta(2) - 4\ln^2 x + \tfrac{44}{3}\ln(1-x) - \tfrac{64}{3}\ln x\} + 8\frac{\ln^2 x}{(1-x)}\\
&\quad + \frac{176}{3}\frac{\ln x}{(1-x)} - \tfrac{184}{9} - \tfrac{1012}{9}x\Bigg]L_M + \Big[\tfrac{44}{3}(1+x)\ln(1-x) + \tfrac{88}{3}x + 44\Big]L_R\Bigg\}\\
&\quad + n_f C_F\Bigg\{\tfrac{4}{3}(1+x)L_M^2 - \tfrac{8}{3}(1+x)L_M L_R\\
&\quad + \Bigg[-\frac{32}{3}\frac{\ln x}{(1-x)} - \tfrac{8}{3}(1+x)\{\ln(1-x) - 2\ln x\} + \tfrac{64}{9} + \tfrac{136}{9}x\Bigg]L_M\\
&\quad + \Big[-\tfrac{8}{3}(1+x)\ln(1-x) - 8 - \tfrac{16}{3}x\Big]L_R\Bigg\}. \qquad \text{(C.7)}
\end{aligned}
$$

In eqs. (2.17) and (2.18) we have presented the scale-independent part of the gg Drell–Yan correction term. The calculation which we have performed also enables us to determine the scale dependence of Δ_{gg}. It is equal to

$$
\begin{aligned}
&\Delta_{gg}(x,Q^2,M^2,R^2)\\
&\quad = \Big[-2(1+4x+4x^2)\ln x - 4(1+2x-3x^2)\Big]L_M^2\\
&\qquad + \Big[-4(1+4x+4x^2)(\mathrm{Li}_2(1-x) + \ln x\ln(1-x)) - 6(1+8x+8x^2)\ln x\\
&\qquad -8(1+2x-3x^2)\ln(1-x) - 15 - 36x + 51x^2\Big]L_M. \qquad \text{(C.8)}
\end{aligned}
$$

Finally, we give the results for the qq, $\bar{q}\bar{q}$ and $q\bar{q}$ (singlet) subprocesses. We find that only Δ_{qq} and Δ_{qq}^{final} have scale-dependent terms (see appendix B for the notation used), viz.

$$\Delta_{qq}(x,Q^2,M^2,R^2) = \frac{N^2-1}{N}\Bigg[\Big\{(1+x)\ln x + \tfrac{1}{2} - \tfrac{1}{2}x + \frac{2}{3}\frac{1}{x} - \tfrac{2}{3}x^2\Big\}L_M^2$$

$$+\Big\{2(1+x)\big(\mathrm{Li}_2(1-x) - \tfrac{1}{2}\ln^2 x + \ln x \ln(1-x)\big)$$

$$+\Big(1-x+\frac{4}{3}\frac{1}{x} - \tfrac{4}{3}x^2\Big)\ln(1-x) + \Big(\frac{4}{3}\frac{1}{x} + 4 - 5x + \tfrac{8}{3}x^2\Big)\ln x$$

$$+\frac{44}{9}\frac{1}{x} - \tfrac{17}{9}x^2 - \tfrac{37}{6} + \tfrac{19}{6}x\Big\}L_M\Bigg] \qquad \text{(C.9)}$$

and

$$\Delta_{qq}^{final}(x,Q^2,M^2,R^2) = \frac{N^2-1}{N^2}\Bigg[2(1+x)\ln x + 4(1-x)$$

$$-\frac{1+x^2}{1+x}\big\{\ln^2 x - 4\ln x \ln(1+x) - 4\,\mathrm{Li}_2(-x) - 2\zeta(2)\big\}\Bigg]L_M\,. \qquad \text{(C.10)}$$

References

[1] R.K. Ellis, *in* Proc. XXIVth Int. Conf. on High energy physics, Munich, August 4–10, 1988, ed. R. Kotthaus and J. H. Kühn, p. 48;
W.J. Stirling, ibid., p. 733

[2] S.G. Gorishny, A.L. Kataev and S.A. Larin, Phys. Lett. B212 (1988) 238

[3] G. Kramer and B. Lampe, Z. Phys. C34 (1987) 497

[4] T. Matsuura, S.C. van der Marck and W.L. van Neerven, Phys. Lett. B211 (1988) 171; Nucl. Phys. B319 (1989) 570

[5] J. Kubar-André and F.E. Paige, Phys. Rev. D19 (1979) 211

[6] G. Altarelli, R.K. Ellis and G. Martinelli, Nucl. Phys. B157 (1979) 461

[7] B. Humpert and W.L. van Neerven, Nucl. Phys. B184 (1981) 225

[8] A.P. Contogouris and J. Kripfganz, Phys. Rev. D20 (1979) 2295

[9] A.N. Schellekens and W.L. van Neerven, Phys. Rev. D21 (1980) 2619; D22 (1980) 1623

[10] M. Diemoz, F. Ferroni, E. Longo and G. Martinelli, Z. Phys. C39 (1988) 21

[11] D.W. Duke and J.F. Owens, Phys. Rev. D30 (1984) 49

[12] E. Eichten, I. Hinchliffe, K. Lane and C. Quigg, Rev. Mod. Phys. 56 (1984) 579 [Erratum: 58 (1986) 1065]

[13] G. Altarelli, M. Diemoz, G. Martinelli and P. Nason, Nucl. Phys. B308 (1988) 724

[14] T. Matsuura and W.L. van Neerven, Z. Phys. C38 (1988) 623

[15] T. Matsuura and W.L. van Neerven, *in* Proc. Int. Europhys. Conf. on High energy physics, Vol. 1, Uppsala, Sweden, June–July 1987, ed. O. Botner (Uppsala University) p. 198
[16] UA2 Collaboration, J. Alitti et al., Measurement of W and Z production cross sections at the CERN $\bar{p}p$ collider, CERN-EP/90-20
[17] CDF Collaboration, Production properties of the W, Z bosons, presented by P.F. Derwent at the 25th Rencontres de Moriond, Les Arcs, Savoie, France (March 1990)
[18] W. Beenakker, F.A. Berends and S.C. van der Marck, program ZSHAPE
[19] A. Denner and T. Sack, ITP-SB-89-52, Z. Phys. C, to be published
[20] P. Aurenche, R. Baier, M. Fontannaz and D. Schiff, Nucl. Phys. B286 (1987) 509; B297 (1988) 661
[21] P. Nason, S. Dawson and R.K. Ellis, Nucl. Phys. B303 (1988) 607; B327 (1989) 49;
W. Beenakker, H. Kuijf, W.L. van Neerven and J. Smith, Phys. Rev. D40 (1989) 54
[22] P. Aurenche and P. Chiappetta, Z. Phys. C34 (1987) 201
[23] P.M. Stevenson, Phys. Rev. D23 (1981) 2916; Nucl. Phys. B203 (1982) 472
[24] A.N. Schellekens, thesis Nijmegen University 1981
[25] A. Erdély, ed., Higher transcendental functions, Vol. 1, Bateman manuscript (McGraw-Hill, New York, 1953);
I.S. Gradshteyn and I.M. Ryzhik, Table of integrals, series and products (Academic Press, New York, 1980)
[26] E.G. Floratos, D.A. Ross and C.T. Sachrajda, Nucl. Phys. B129 (1977) 66 [Erratum: B139 (1978) 545];
A. González-Arroyo, C. López and F.J. Ynduráin, Nucl. Phys. B153 (1979) 161;
E.G. Floratos, P. Lacaze, C. Kounnas, Phys. Lett. B98 (1981) 285